university of groningen / faculty of mathematics and natural sciences

incas^3

Cochlear mechanics: Extension of the circuit model to the middle ear

Oscar Heslinga

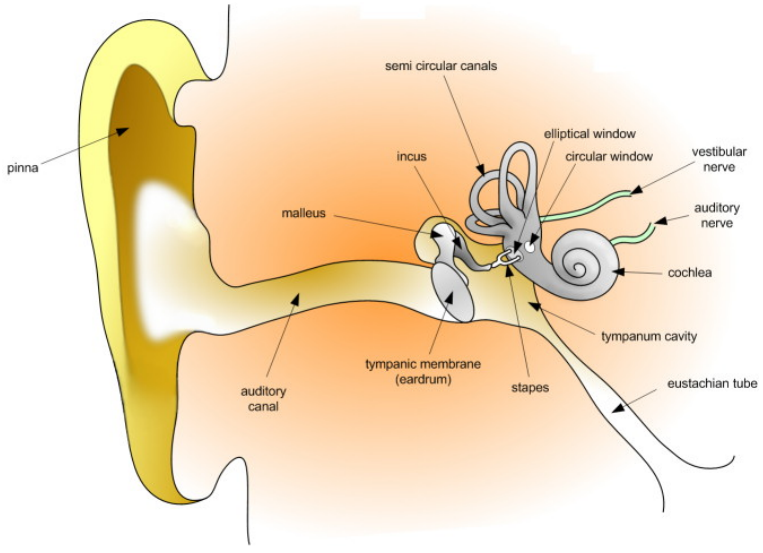

Master Thesis in Applied Mathematics

December 2013

Cochlear mechanics: Extension of the circuit model to the middle ear

Summary

The circuit approach of the cochlea model written out by van den Raadt has been reconsidered to extend the circuit for the middle ear. The middle ear model of O'Connor and Puria has been coupled and the equations of motion are derived in the same structure. Differences in model elements of the middle ear cause singularities which prohibit the original explicit time integration to solve the equations of motion. Inspired by equivalent problems in fluid mechanics, an implicit time integration method has been chosen that resolves the problem of singularity. The original cochlea model has been rewritten in implicit structure and verified with results from the explicit version of INCAS^3. The middle ear model is built with an implicit time integration and verified with results from O'Connor and Puria. After coupling of the two model parts, simulations are made to study the effect of the new model and a nonlinear damping function is implemented to show the capabilities to simulate active behaviour of the cochlea considering future research on otoacoustic emissions.

Keywords: cochlear mechanics, middle ear, implicit time integration, nonlinear damping

Master Thesis in Applied Mathematics
Author: Oscar Heslinga
Supervisor: prof. dr. A.E.P. Veldman
Second supervisor: prof. dr. E.C. Wit
External supervisor: dr. ir. P.W.J. van Hengel
Date: December 2013

Institute for Mathematics and Computer Science
P.O. Box 407
9700 AK Groningen
The Netherlands

Contents

1 Introduction **1**

2 Anatomy and function of the human ear **3**
2.1 Anatomy . . . 3
2.2 Functionality of the cochlea . . . 4
2.3 Why study the cochlea? . . . 5
2.3.1 Otoacoustic emissions . . . 6
2.3.2 Cochlear implants . . . 7
2.3.3 Sensor development . . . 7

3 Cochlear Modeling **9**
3.1 Assumptions . . . 9
3.2 A one-dimensional model . . . 10
3.3 The discrete 1D-model . . . 14
3.4 The electrical analagon of the 1D-model . . . 17
3.4.1 Basic electronics . . . 18
3.4.2 The circuit model of the cochlea . . . 19
3.5 Overview . . . 25

4 Extension to the middle ear **29**
4.1 Why study and improve the model for the ME? . . . 29
4.2 Physiology of the ME and O'Connor and Puria's circuit model . . . 30
4.3 Extension of the circuit equations . . . 33
4.4 The implicit cochlea model . . . 34
4.5 Differential algebraic equations . . . 39
4.6 Results . . . 41
4.6.1 The amplitude envelope . . . 43
4.6.2 Artificial diffusion . . . 45

5 The implicit middle ear model **49**
5.1 Circuit model and equations . . . 49
5.2 Results . . . 52
5.3 Adding the cochlea to the ME . . . 55
5.4 Implementation of nonlinear damping . . . 58
5.4.1 Active behaviour . . . 61

6 Conclusion and future research **65**

A Tables of constants and parameters **67**

B Matrices for the implicit total ear model **69**

C Matlab code of the developed models **71**

Chapter 1

Introduction

The knowledge of the human inner ear, the cochlea, has been developing for over several centuries. In the 1980s, modeling techniques and tools started to evolve and problems started to leave the biological sense and stretch towards the field of mechanics. By observing the cochlear mechanics in great detail one could say that it is an outstanding piece of engineering by the human body with complex functionalities that are responsible for digesting sound from the environment. To develop a model describing the complexities of cochlear mechanics, the departments of Biophysics and Applied Mathematics of the University of Groningen cooperated in the development of a numerical model, the cochlea model described in van den Raadt [4] and Duifhuis [5]. The Institute for Control Systems and Sensor Systems (INCAS^3) in Assen, the Netherlands is in possession of a cochlea model and performs research on the improvement. This thesis is inpsired by the research ideas at INCAS^3.

One of the most fascinating features of the cochlea is its ability to produce emissions of sound. Using common sense, we would consider the cochlea as a passive device recording emissions from the environment and reporting its analysis to the brain. Deeper research however, shows that the cochlea also has an active part that allows the cochlea to produce an emission as a response to an external emission and surprisingly also spontaneous. These emissions are called (spontaneous) otoacoustic emissions. Since otoacoustic emissions are produced within the cochlea itself, they provide an objective method to test the cochlea in hearing screenings [12].

Otoacoustic emission measurements can be performed by placing a microphone and receiver in the earcanal. The receiver produces acoustic stimuli and the microphone receives the response out of the cochlea. Placing it in the ear canal reduces many environmental influences but we cannot get closer to the cochlea and we will always have to deal with the effect of the middle ear. In the existing cochlea model, the middle ear model is a crude simplification and there is much space for improvement. Moreover, the otoacoustic emissions are of very low amplitude so every form of noise from the environment should be lowered to the minimum to recognize the active behaviour of the cochlea. Therefore, a proper model of the middle ear is necessary.

A more detailed model, in an analagous modeling structure as the cochlea model, has been presented recently by O'Connor and Puria [1] and matches experimental data quite

well. The goal for this thesis is to link the new middle ear model to the cochlea model. The coupling must not affect the capabilities of the present model in simulating active behaviour of the cochlea in the aim of studying otoacoustic emissions. Therefore, after coupling, the model should be verified extensively with results achieved before. Eventually, a more detailed middle ear model would improve our knowledge of the behaviour of the human ear and contribute in many audiological applications.

Section 2 presents an overview of the physiology of the human ear to build up some terminology and explains the functioning of the cochlea qualitatively. This is followed by the derivation of the cochlea model and the method to solve the model equations in section 3. The middle ear model is coupled in section 4 and we encounter problem of the time integration of the new model equations. An implicit time integration method instead of an explicit one is presented for the cochlea and middle ear, which solves the problem of solving the model equations. Finally, section 5 presents results of the validation with the middle ear model of [1] and simulations in detecting active behaviour of the cochlea.

Chapter 2

Anatomy and function of the human ear

We start with providing some pictures and terminology to just get a feeling of the environment we will study. The functionality of the cochlea is described qualitatively and we distinguish the essential elements we have to study in more detail to come up with a mathematical model. Also some medical applications are presented to support the importance of a suitable cochlea model.

2.1 Anatomy

The main function of the human ear is receiving sound waves and report to the brains what it is perceiving. A good way to study the anatomy and functionality of the human ear is just to follow an incoming sound wave on its way through the complex structures of the ear. An overview of the basic elements of the ear is given in figure 2.1 and will be used as reference for terminology.
A sound wave enters the ear at the auditory canal, or simply ear canal, where it has to pass through the ear drum. Probably this is the point where the knowledge on ears of an average person ends and where we will continue. The ear drum is the separation of the region called the outer ear with the middle ear (ME). It is set in motion by the incoming sound wave due to pressure change in the air. The ear drum is attached to a chain of ossicles called malleus, incus and stapes. The translation from Latin is hammer, anvil and stirrup, respectively. Their names can be deduced from the figure with a little creativity. The displacement of the ear drum is mechanically transported by the chain of ossicles to end at the stapes. This ossicle is connected to the right with the oval window (OW) which is the border of the ME with the inner ear. The most important part of the inner ear and for hearing, is the cochlea, a tube filled with fluid which is coiled in the shape of a snail shell. The beginning at the OW is called the base and the end the apex which lie approximately 35 mm from each other. The cochlea is responsible for the translation of mechanical processes to electrical signals through its connection with the nerves. So how does this translation work?

The cochlear tube is further specified in figure 2.2. In this cross section of the tube we see that it is divided in three chambers; the scala vestibuli (SV), the scala media

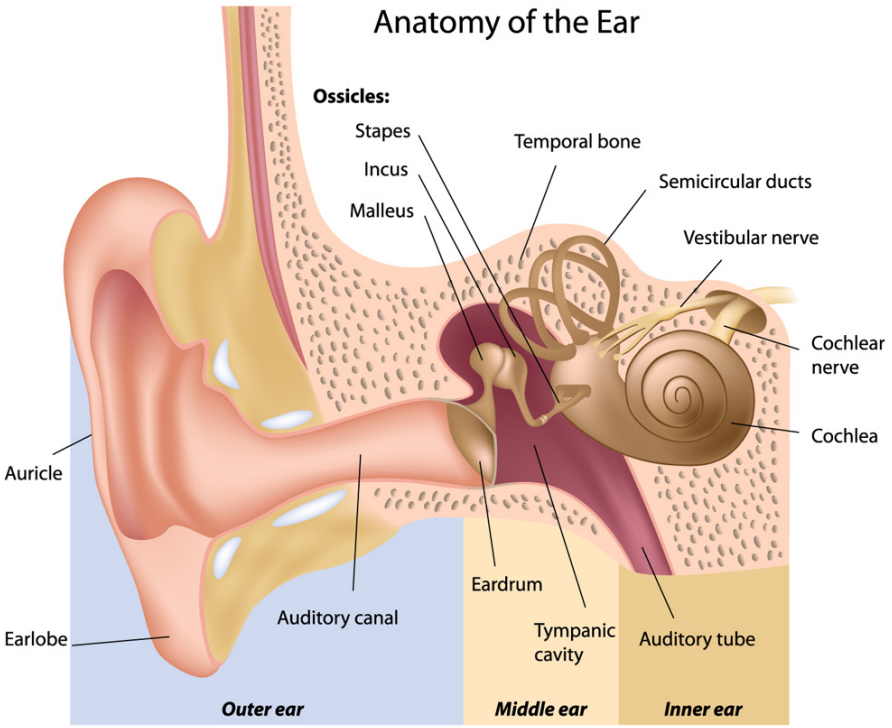

Figure 2.1: Anatomy of the human ear

(SM) and the scala tympani (ST). The SV and ST are filled with perilymph, the cochlear fluid, and are separated by the SM. However, at the apex, there is a small hole called the helicotrema where fluid flow between the SV and ST is possible. The SM is filled with fluid called endolymph and together with Reissner's membrane and the basilar membrane (BM) it forms the cochlear partition (CP).
Within the CP we have the Organ of Corti where the hair cells are situated. The bundles of hair cells are covered by the tectorial membrane and are responsible for reading the mechanics and passing the information to the nerves. The interaction of the tectorial membrane, the Organ of Corti and the hair cells is a very complex process which will not be studied in more detail. It is assumed that the SM and the other elements in the CP do not affect the mechanics of the cochlea. The main lesson is to treat the CP as a membrane containing hair cells and separating the SV from the ST.

2.2 Functionality of the cochlea

The oval window (OW) transports the mechanical energy from the ME ossicles into the SV. The ST has a round window (RW) located at the entrance of the cochlea. The transport of energy causes pressure change within the fluid chambers initiating displacement of the CP. So how is the cochlea capable of identifying sound and translating this into electric signals?

It was already mentioned that the fabrics responsible for this process are the hair cells.

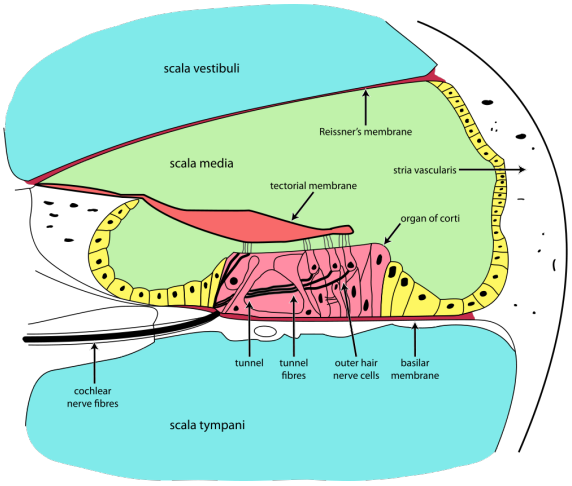

Figure 2.2: Cross section of the cochlear tube

There are two types of hair cells; the inner hair cells (IHCs) and outer hair cells (OHCs). The hair cells are covered by the tectorial membrane. Changes in fluid pressure in the SV and ST cause the elements in the CP to move and therefore the IHCs. Stimulation of a bundle generates a potential which leads to an electric signal in the underlying nerve cell. Via the auditory nerves this is transported to the brain. The OHCs have a different, more undiscovered function. Fact is that OHCs contribute to the functioning of the cochlea. OHCs are able to change length when a pressure or electric field is varied, this is called motility. This motility has a relation with the property of the cochlea to damp high levels of sound to protect itself and reversely amplify low levels of sound to make them detectable. However, the mechanics behind this process is not clear [2] and these are details that do not have to be considered for the micromechanics of the CP.

The mechanical parameters (mass, damping and stiffness) of the CP vary along the length of the cochlea. A stimulus that travels along the CP causes the membrane to resonate at a certain point. This is called the characteristic place regarding this frequency. Here, the displacement of the membrane will be at its maximum. The connecting IHCs will be triggered and send a nerve signal to the brains reporting that the frequency belonging to this characteristic place has been sensed. Throughout the cochlea every frequency (within the human aural range) has a characteristic place. This is called the frequency-place map. High frequencies at the base and low frequencies at the apex. The relation between the frequency f and place x is nonlinear. This has to do with the aforementioned property to deal with a broad range of amplitudes and frequencies. A visualization of the resonance process of the CP is given in figure 2.3.

2.3 Why study the cochlea?

The functioning of the cochlea is explained very briefly. We can build on this knowledge to derive a quantitative model. But, besides our natural curiosity, why would we develop a so called **cochlea model**? There are some nice industrial applications which benefit from a quantitative understanding of the cochlea which we will study briefly but the main

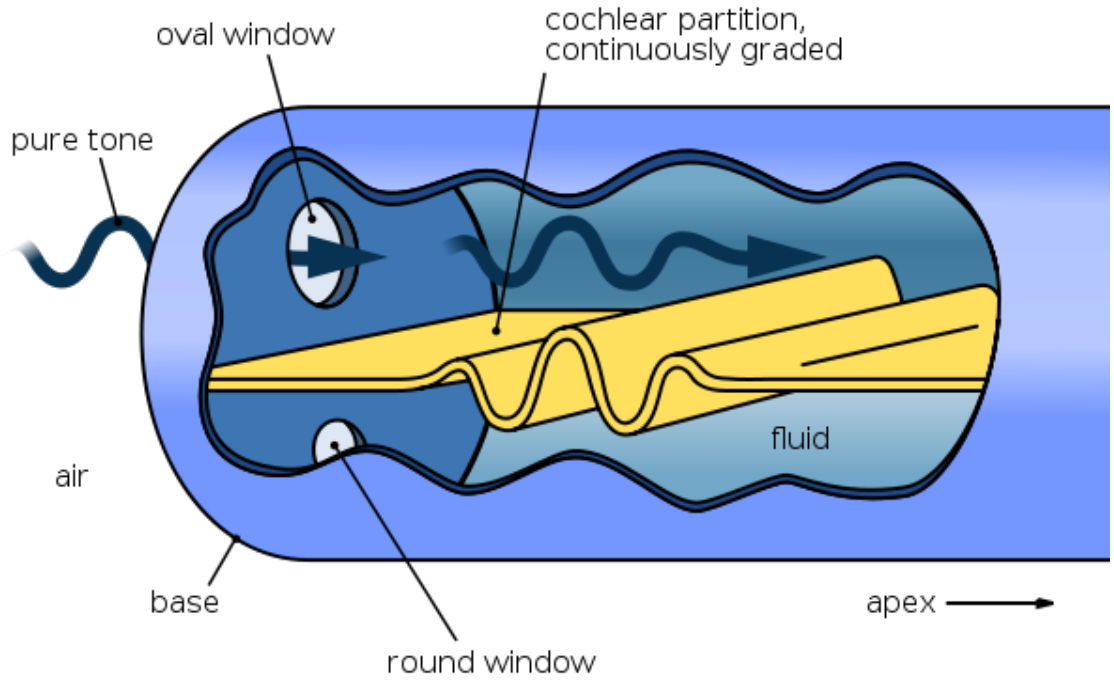

Figure 2.3: The cochlea represented as a tube with fluid and the CP as a membrane. When a pure tone finds its way through the cochlea, the membrane will resonate at the characteristic place giving maximum amplitude.

application area is in improving diagnostics and revalidation for the hearing impaired.

2.3.1 Otoacoustic emissions

One of the most interesting features of the cochlea is that it is able to produce sound and send this to the outside world. These self generated sounds are called otoacoustic emissions (OAEs). OAEs are generated as a response to an incoming stimulus. However, it is even possible to measure emissions without an evoking stimulus. This subgroup of OAEs is called spontaneous otoacoustic emissions (SOAEs) and hence these emissions occur spontaneously. One should realize that these emissions are only detectable by highly sensitive microphones plugged into the ear canal with not even the smallest bit of noise from the environment.

The clinical application of OAEs is that such emissions can indicate whether a cochlea is healthy or not. If we present a stimulus to a patient and measure the evoked OAE we can compare the result with OAEs from a healthy cochlea. This gives us an objective testing method to determine whether the patient has a hearing deficit, specifically in the cochlea. At the moment the only alternative is just asking whether a patient hears a specific stimulus. A disadvantage of this test is the level of subjectivity and we depend on the assessment skills of the patients. Moreover, we cannot distinguish whether the hearing deficit lies in the cochlea or somewhere else in the hearing system. With regard

to the subjectivity problem, infants are not capable of answering these questions. An objective testing method allows us to diagnose hearing deficits at a very young age and start necessary procedures earlier. Having a good understanding of cochlear mechanics is essential for developing such a method.

2.3.2 Cochlear implants

A cochlear implant is an artificial cochlea for humans who do not possess a functional cochlea themselves. A microphone is placed at the outside of the skull and an implant transforms the incoming sound to electric signals which are sent to the auditory nerve through an electrode, see figure 2.4.

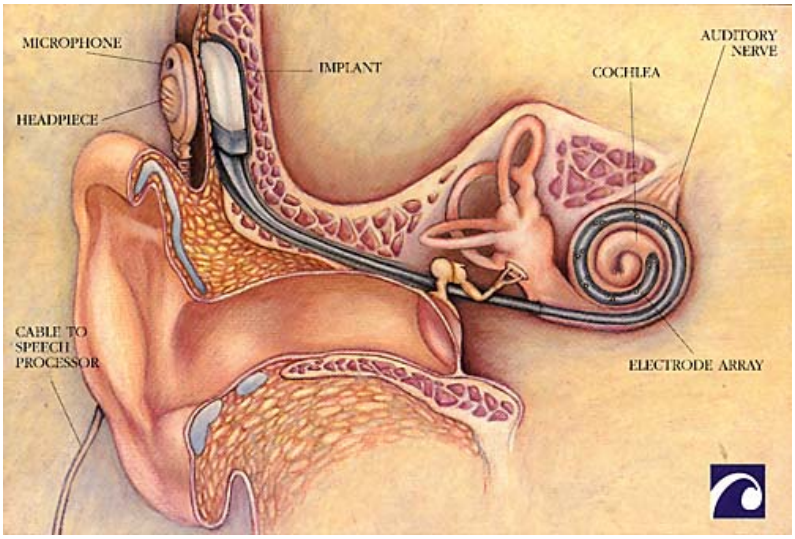

Figure 2.4: Figure of a human ear where a cochlear implant has been placed

The implant needs to imitate the function of the cochlea which is a very complex process. The healthy cochlea is able to distinguish around ten thousand frequencies. A performance that is not feasible for an artificial cochlea with the current surgical techniques delivering such high resolution signals electrically to the cochlear nerve. However, with a set of a few electrode contacts at essential frequencies, completely deaf patients are able to perceive and learn speech to an acceptable level, young children in particular. To develop and improve this device, a reliable cochlea model would be very useful. Future improvements could lead to the ability for deaf patients to perceive sound better, for instance music which is not possible so far, and improve life quality.

2.3.3 Sensor development

A good example of research where the cochlea model is applied is the field of sensor systems. Basically, a sensor can be seen as a device which measures a certain physical quantity. The coupled system analyzes the measurement and outputs a signal to the environment. These signal data assist the environment in taking decisions. For example, when a person perceives the sound of an approaching car, the cochlea system identifies the frequencies and amplitudes belonging to sound of an approaching car and sends this

information to the brains. By experience from previous situations, the human brain decides whether danger is on the lurk and takes action. How do we develop a sensor system that warns a deaf person to step away from the road? Can we use sound to determine whether a patient is in need of help if the person is physically not able to press a button? How to classify sound with such a precision that situations that require action and dangerless situations are distinguished well? These kind of questions can be answered basically by understanding and imitating the perceivement skills of the human body. From the perspective of sound, the development and improvement of the cochlea model is essential to develop software for sensor systems.

Chapter 3

Cochlear Modeling

In the following chapter we use the anatomical knowledge of the cochlea to set up a mathematical model. The construction of such a model requires a lot of assumptions which could lead to a model that does not represent nature anymore. In making each assumption, we should be very careful in the trade-off between the representation of a natural cochlea and being able to cope with the mathematics and solvability of the model. We will describe the one-dimensional cochlea model as presented by van der Raadt in [4].

3.1 Assumptions

First it is necessary to describe how we come from the anatomical description of the cochlea to a one-dimensional model still containing the essential mechanics of the cochlea. Therefore, we make a list of assumptions specified in [2].

- The ear is placed in an infinite space containing only air. There are no external influences from outside the ear except for the mechanical properties of the surrounding air.
- The existence of the ear canal is neglected.
- For now, the ME is treated as a mechanical bandpass filter which transforms incoming displacement and pressure difference in air to that in the cochlear fluid through an impedance match. Later in this thesis we study the modeling of the ME in more detail.
- The cochlear windows (the OW and RW) are assumed to be open and have no mechanical properties influencing the incoming signal. Of course , these windows might have these properties because they are an existing piece of tissue in the ear. We assume that properties of the OW are incorporated in the ME. For the RW this is not possible but we neglect its influence until this is proven wrong.
- As described earlier, the cochlea is a rolled circular tube decreasing in diameter. For modeling purposes we roll out this tube and assume the shape to be rectangular and constant in cross-section. It is shown that these assumptions do not cause a lot of loss in accuracy [2]. Furthermore, we are only interested in the longitudinal direction of the cochlea which rectifies the assumption for the rectangular cross-section.

- The cochlear fluid is assumed to be uniform: there is no difference in concentration or chemical composition of the fluid throughout the cochlea.
- The fluid is incompressible, linear and inviscid: the density of the fluid is constant and there are no transport phenomena like resistance, turbulence or stress.
- The CP is treated as only the basilar membrane so mechanics due to Reissner's membrane, the Organ of Corti and the SM are neglected. The BM is a row of unconnected segments coupled through interaction through the surrounding fluid.

So what is now left at the end of all our assumptions? The geometry of the cochlea model we are going to work with is given in figure 3.1. It is now time te define variables, parameters and mechanical equations to set up a mathematical model for the cochlea.

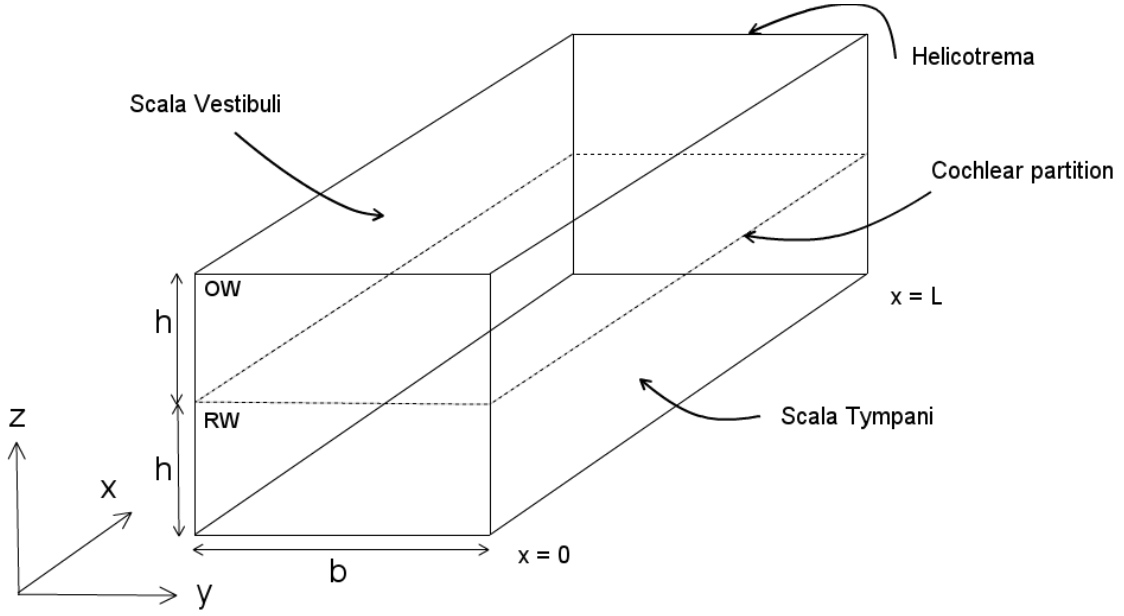

Figure 3.1: Geometry of the cochlea

3.2 A one-dimensional model

As described above, the cochlea is modeled as a straight, two chambered box as suggested by Viergever [6] given in figure 3.1. The upper chamber represents the SV and the lower the ST separated by the CP. The walls of both chambers are rigid at each side except at the OW and RW where the ME performs a transition from fluid to the outside air. Of course the CP is also not rigid and can displace due to pressure differences and fluid displacement. The longitudinal direction lies along the x-axis with the ME at $x = 0$. The apex is the helicotrema at $x = L$, which is the length of the cochlea. Throughout the whole length it is assumed that the width (the y-direction) of the CP is b, a constant independent of x. The height (the z-direction) of the SV and ST are assumed equal and constant h with the CP at $z = 0$.

We are interested in the way the cochlea responds on an incoming stimulus. When a stimulus enters the SV at the OW two phenomena occur.

- Fluid will displace because of the pressure difference initiated by the stimulus
- Displacement in the cochlear fluid yields a pressure difference in the fluid that causes the CP to move.

The goal is to model this mechanical behaviour and solve variables like the velocity and pressure in the fluid and the displacement of the CP.

Start with the first phenomenon, the flow of cochlear fluid. As usually in problems in Computational Fluid Dynamics (CFD) conservation laws are derived. Since we work towards a one-dimensional model we are only interested in the x-direction. Consider figure 3.1 and take a slice of the SV and the ST with thickness ΔX, see figure 3.2.

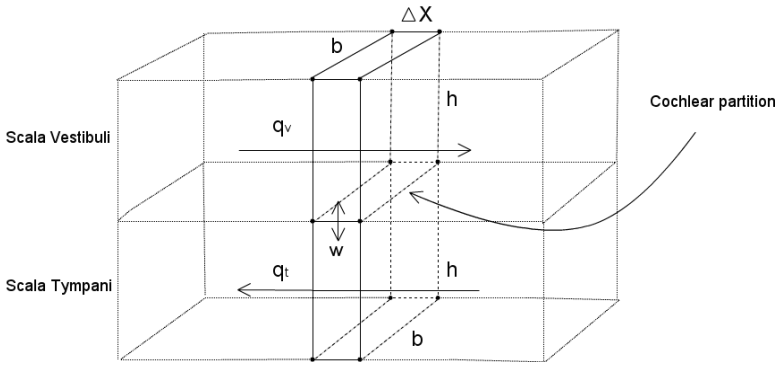

Figure 3.2: A slice of width ΔX with a visualization of the transpartition velocity w and volume flux q_v and q_t

The cross sectional area of both chambers is $A_v = bh$. We represent the flow with the flux q; the amount of volume that has been transported per second through a surface (the cross-sectional area), hence the unit of flux is $\frac{m^3}{s}$. Consider a flux q_v through a slice of the SV. Then the difference of the fluxes at both ends is the transpartition velocity , the velocity which the CP is moving in the y-direction, represented by an average point velocity $w(x,t)$. Conservation of mass gives us:

$$w(x,t)b\Delta X = q_v(x+\Delta X,t) - q_v(x,t) \tag{3.1}$$

Divide both sides by ΔX and let $\Delta X \to 0$ and we find:

$$w(x,t)b = \frac{\partial q_v(x,t)}{\partial x} = A_v \frac{\partial u_v(x,t)}{\partial x} \tag{3.2}$$

We assume that u_v is small and hence in the conservation of momentum (the Euler equation) in x-direction the convective term disappears:

$$\frac{\partial u_v}{\partial t} + u_v \frac{\partial u_v}{\partial x} = -\frac{1}{\rho}\frac{\partial p_v}{\partial x} \Longrightarrow -\rho \frac{\partial u_v}{\partial t} = \frac{\partial p_v}{\partial x} \tag{3.3}$$

Now it is time to study the mechanical activity of the CP better. Due to the transpartition velocity a force is exerted on the membrane. But how can we connect force with velocity? The coupling between these two properties is called the mechanical impedance Z. Z is the ratio between force and velocity and is a measure of how much opposition a velocity will face when created by a force. This can be generalized as follows. When a certain potential difference acts on a system, this system will resist against this change of state. The resistance is generally called impedance and is specified by the properties of the system. In this case the system is the membrane which is resistive because of its elastic properties. In an electrical wire the potential difference is the voltage which creates a current of electrons. These electrons will face a resistance, the electrical impedance, on their way through the wire. Equally, when a sound pressure is applied in a fluid, a flux will be initiated (mentioned earlier as q_v) to transport the acoustic energy. Pressure and flux are connected via the acoustic impedance. The pressure in both the SV and ST, p_v and p_t respectively, are set to zero in the rest position of the membrane (of course there is a reference pressure p_{ref} in both chambers but only the difference $p_v - p_t$, where p_{ref} disappears is of interest). p_v and p_t are equal with different sign since they are connected through the membrane, such that $p_v = -p_t$. There is a force balance at the CP. At the LHS of (3.4) the pressure of the fluid (which is force per area) and at the RHS the force (velocity $\times$ impedance) pointing in the other direction. Z_{CP} is the specific acoustic impedance (which is mechanical impedance per unit area).

$$p_v(x,t) - p_t(x,t) = 2p_v(x,t) = -w(x,t)Z_{CP}(x) \tag{3.4}$$

We are only left with the elastic properties of the CP. The CP is modeled as a row of N oscillators representing the hair cells on the BM. These oscillators have a mass, damping and stiffness and are driven by the pressure force explained above. To understand the choice for oscillators we make a short step to basic theory of mechanical oscillators.

Normally in mechanics, we use Newton's second Law;

$$F = ma \tag{3.5}$$

with mass m $[kg]$ and acceleration a $[\frac{m}{s^2}]$. Acoustics appear in fluids through differences in pressure and therefore it is common to refer to pressure p instead of force F. Pressure is a force per unit area A, so (3.5) in terms of pressure is derived by dividing both sides by A.

$$p = m^s a \tag{3.6}$$

Where m^s $[\frac{kg}{m^2}]$ the specific acoustic mass. The same for specific acoustic damping d^s and stiffness s^s which have unit $\frac{kg}{m^2}$, $\frac{kg}{m^2 s}$ and $\frac{kg}{m^2 s^2}$ respectively. Specific acoustic variables are indicated with a superscript s.

For a pressure p the mechanical oscillator is modeled by the following ODE:

$$p = m^s \frac{\partial^2 y}{\partial t^2} + d^s \frac{\partial y}{\partial t} + s^s y = p_0 \cos(\omega t) \tag{3.7}$$

where y is the displacement and m^s, d^s and s^s specific acoustic mass, damping and stiffness .

The solution of (3.7) is given by:

$$x(t) = \frac{p_0}{|Z_a|\omega}\sin(\omega t - \phi), \text{ with } Z_a = d + i\left[\omega m - \frac{s}{\omega}\right] \text{ and } \phi = \arctan\left[\frac{1}{d}\left(\omega m - \frac{s}{\omega}\right)\right] \tag{3.8}$$

Z_a is the acoustic impedance of the cochlear fluid. It is a complex function with an imaginary part that vanishes when $\omega = \omega_0 = \sqrt{\frac{s}{m}}$. This ω_0 is called the resonance frequency. At $\omega = \omega_0$, Z_a equals the damping d and the size of $|Z_a|$ reaches a minimum. Hence, with this minimal damping the displacement x will be maximal. Over the whole CP there are N oscillators which vary in damping and stiffness and therefore each oscillator has its own resonance frequency. Hence, the function of the CP is modeled. An external pressure wave will have a frequency which will be the resonance frequency of one of the oscillators at the CP. The mechanism to detect sound and to identify its frequency.
To indicate whether d is small compared to m and s (to indicate the amplitude at resonance) we define the damping factor $\delta = \frac{d}{\sqrt{ms}}$. A good damping gives a sharp response, i.e. in the frequency domain a peak with a high amplitude and small width.
So for each section we can set up the standard model for a harmonic oscillator from mechanics:

$$-w(x,t)Z_{CP}(x) = m^s(x)\frac{\partial^2 y}{\partial t^2}(x,t) + d^s(x)\frac{\partial y}{\partial t}(x,t) + s^s(x)y(x,t) \tag{3.9}$$

$y(x,t)$ is the displacement of the membrane caused by the pressure, so $w(x,t) = \frac{\partial y}{\partial t}(x,t)$. Furthermore, the mass m^s, damping d^s and stiffness s^s are dependent of x because each row of hair cells has its own properties.

$$-w(x,t)Z_{CP}(x) = m^s(x)\frac{\partial w}{\partial t}(x,t) + d^s(x)w(x,t) + s^s(x)\int w(x,t)dt \tag{3.10}$$

Head back to (3.2) and differentiate both sides with respect to t.

$$b\frac{\partial w}{\partial t} = A_v\frac{\partial^2 u_v}{\partial x \partial t} \tag{3.11}$$

Plug in the Euler equation of (3.3) to substitute $\frac{\partial u_v}{\partial t}$.

$$-\frac{\rho b}{A_v}\frac{\partial w}{\partial t} = \frac{\partial^2 p_v}{\partial x^2} \tag{3.12}$$

Substitute (3.4) for the emerging p_v (for the sake of simplicity the x and t-dependency of the functions is omitted):

$$\frac{2\rho}{h}\frac{\partial w}{\partial t} = \frac{\partial^2}{\partial x^2}\left(-wZ_{CP}\right) = \frac{\partial^2}{\partial x^2}\left(m^s\frac{\partial w}{\partial t} + d^s w + s^s\int w dt\right) \tag{3.13}$$

Equation (3.13) is a PDE for w but if we are interested in the displacement of the membrane we can substitute $w(x,t) = \frac{\partial y}{\partial t}(x,t)$ and integrate both sides to t to find the same PDE for y. These modifications are justified under the assumption that $w(x,t)$ and $y(x,t)$ have sufficient properties concerning differentiability.

$$\frac{\partial^2}{\partial x^2}\left(m^s\frac{\partial^2 y}{\partial t^2}+d^s\frac{\partial y}{\partial t}+s^s y\right)-\frac{2\rho}{h}\frac{\partial^2 y}{\partial t^2}=0 \tag{3.14}$$

We go one step further by considering the flux q instead of velocity w. In (3.2) the concept of flux was explained to be the quantity of fluid flowing through a surface A and hence $q = Aw$ $[\frac{m^3}{s}]$. It depends on the direction of q which surface A we are dealing with. In case of the cochlea, the flux q on the CP is in the y-direction on the surface $A = b\Delta X$. The fluid flux in the SV in contrary would consider the surface $A_v = bh$ (see figure 3.2). The model of (3.13) will be solved for q instead of w and therefore we subsititute $w = \frac{q}{A}$ in this equation .

$$\frac{2\rho}{Ah}\frac{\partial q}{\partial t}=\frac{\partial^2}{\partial x^2}\left(m\frac{\partial q}{\partial t}+dq+s\int q dt\right) \tag{3.15}$$

The one-dimensional model (3.15) is named the 'coupled oscillator model'. At the LHS of (3.15) logically q emerges. At the RHS the division by A is included in the parameters m, d and s , the acoustic mass, damping and stiffness with units $[\frac{kg}{m^4}]$, $[\frac{kg}{sm^4}]$ and $[\frac{kg}{s^2m^4}]$ respectively. Up to this point, m represented the regular 'mechanical' mass in kg but from now now on we work purely with acoustic masses. The different acoustic parameters will be treated in the next section.

3.3 The discrete 1D-model

To solve the model of (3.15) numerically we will set up a computational grid and discretize the model equations. The corresponding figure is figure 3.3.

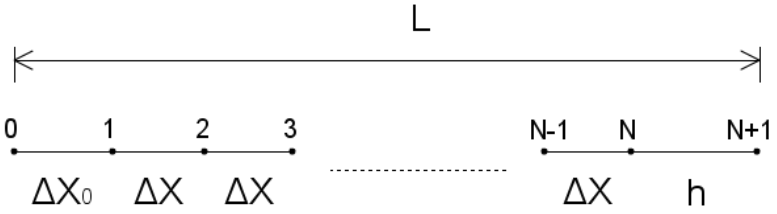

Figure 3.3: The grid for the cochlea in the x-direction

The total cochlea has length L and is divided in N sections. The position of the i-th section is located at x_i and the width of a section is ΔX. Some exceptions are made at the boundaries. The most right section has width h because the helicotrema is situated here and we want to let the grid correspond with figure 3.4. On the other side, the most left section has width ΔX_0. This has to do with the fact that the distance between two oscillators ΔX could differ from the distance of the first oscillator to the ME. From figure 3.3 we conclude:

$$\Delta X_0 + N\Delta X + h = L \tag{3.16}$$

For the time interval in which we want to solve the equations, define the interval $[t_0, t_{end}]$ and take a timestep Δt such that each point in time $t^{(j)} = j\Delta t$ is defined.

Each section has an acoustic mass, damping and stiffness parameter which we will study in more detail. As mentioned in the previous section, the parameters depend on the direction of the dynamics. First, we will treat every parameter present in the cochlea.

- $\underline{m_n}$ is the acoustic mass of the membrane at the n-th position in the cochlea. It is calculated by the specific acoustic mass of an oscillating hair cell (constant throughout the cochlea) on a slice $b\Delta X$ on the membrane.

$$m_n = \frac{m^s}{b\Delta X} \tag{3.17}$$

- $\underline{m_c}$ is the mass of the cochlear fluid and determined by the slice of fluid with length ΔX and the geometry of the SV and ST which is A_v.

$$m_c = \frac{\rho A_v \Delta X}{A_v^2} = \frac{\rho \Delta X}{A_v} \tag{3.18}$$

  Note that m_c and m_n have different areas, A_v and $b\Delta X$ respectively, that convert the mechanical masses $[kg]$ to acoustic masses $[\frac{kg}{m^4}]$. This is because m_c is the mass term belonging to the fluid in the SV and ST (x-direction, surface $A_v = bh$) and m_n belongs to the oscillatory dynamics of the CP (y-direction, surface $b\Delta X$). P

- $\underline{m_{c0}}$ follows the same story as for m_c except that the oscillator distance ΔX could be different at the first section.

$$m_{c0} = \frac{\rho A_v \Delta X_0}{A_v^2} = \frac{\rho \Delta X_0}{A_v} \tag{3.19}$$

  This feature of the model is not of interest for our research and therefore ΔX_0 is assumed to be equal to ΔX. The result is that m_{c0} equals m_c but we keep m_{c0} in the upcoming equations to see where it would appear.

- $\underline{m_h}$, the acoustic mass at the helicotrema can be derived by considering the geometry of the helicotrema in more detail, see figure 3.4. We assume the helicotrema as a circular tube coiling around the CP. It has radius h so it connects perfectly with the geometry of the SV and ST. Figure 3.4 only gives a side view but the width of the helicotrema in y-direction is given b (just as the rest of the cochlea). The unit area on which the pressure is acting is still A_v, so the acoustic mass is:

$$m_h = \frac{\rho\left(\frac{\pi}{2}h^2 b\right)}{A_v^2} = \frac{\pi\rho}{2b} \tag{3.20}$$

- $\underline{m_m}$, $\underline{d_m}$ and $\underline{s_m}$ are the parameters representing the ME. These are explained together because of their relations from the theory on mechanical oscillators. The ME should be modeled with the important feature that we make the transition from cochlear fluid to air. The first oscillator is situated at $n = 1$ and the mechanisms belonging to the ME at $n = 0$. The transition of air to cochlear fluid is modeled as a transformator. A transformator transforms an incoming stimulus by a transformation factor n_t. The pressure p_{in} of an input stimulus is transformed to $p_{out} = n_t p_{in}$

and the velocity u_{in} becomes $u_{out} = \frac{u}{n_t}$. In this way, the energy E (proportional to the product of p and u) of the incoming and outgoing stimulus is equal because:

$$E \propto p_{out}u_{out} = (n_t p_{in})\left(\frac{u_{in}}{n_t}\right) = p_{in}u_{in} \tag{3.21}$$

Consider a stimulus that approaches from the ear canal. It brings an external pressure p_e and a velocity u_e. This stimulus has to find its way through air which has a characteristic impedance Z_a (given in the Appendix), so $Z_a = \frac{p_e}{u_e}$. With a transformation factor n_t the transformed pressure and velocity are $n_t p_e$ and $\frac{u_e}{n_t}$ and the new impedance reads:

$$Z = \frac{n_t p_e}{\frac{u_e}{n_t}} = n_t^2 Z_a \tag{3.22}$$

Z has unit $\frac{kg}{sm^4}$ and as presented in section 3.2 its real part is equal to d (see (3.8)) so therefore $d_m = n_t^2 Z_a$. In this section we also introduced the relation $\delta_m = \frac{d_m}{\sqrt{m_m s_m}}$ (in case of the ME oscillator). The damping factor δ_m is a given parameter and ω_{rm} is the resonance frequency of the ME. The values of these parameters are known from acoustic standards and can be found in the Appendix.

$$\omega_{rm} = \sqrt{\frac{s_m}{m_m}} = \sqrt{\frac{s_m m_m}{(m_m)^2}} \Longleftrightarrow \omega_{rm} m_m = \sqrt{s_m m_m} \tag{3.23}$$

Use the relation between δ_m and d_m to find:

$$\frac{d_m}{\omega_{rm} m_m} = \delta_m \Longrightarrow m_m = \frac{d_m}{\omega_{rm}\delta_m} = \frac{n_t^2 Z_a}{\omega_{rm}\delta_m} \tag{3.24}$$

And the same idea for finding s_m:

$$\omega_{rm} = \sqrt{\frac{s_m}{m_m}} = \sqrt{\frac{(s_m)^2}{m_m s_m}} = \frac{s_m \delta_m}{d_m} \Longrightarrow s_m = \frac{d_m \omega_{rm}}{\delta_m} = \frac{n_t^2 Z_a \omega_{rm}}{\delta_m} \tag{3.25}$$

The specific impedance of air Z_a^s is a given parameter in acoustics (see Appendix) and Z_a is calculated by scaling with the given area of the ear drum A_t so $Z_a = \frac{Z_a^s}{A_t}$.

The final properties that we have to specify is the value of the damping and stiffness of the hair cells. For the damping d_i and stiffness s_i at the i-th oscillator in the cochlea there are different choices. The stiffness s_i is modeled by a continuous function $s(x)$ so $s_i = s(x_i)$ (x_i is the position of the i-th oscillator).

$$s(x) = \frac{s_0^s}{b\Delta X} e^{-\lambda x} \tag{3.26}$$

λ is a parameter based on experiments and s_0^s is the specific acoustic stiffness constant (given in the Appendix). It is the stiffness of hair cells so the area converting s_0^s to the acoustic stiffness is $b\Delta X$.

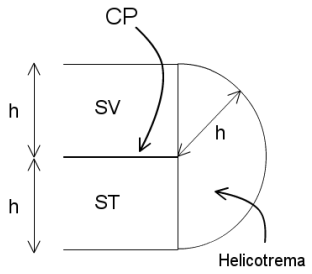

Figure 3.4: The geometry of the helicotrema

With $s(x)$ we can also derive the frequency-place map mentioned in section 2 of a resonance frequency f_r and the position x on the BM of the triggered hair cell. Use the relation for resonance frequency from the mechanical oscillator and $\omega_r = 2\pi f_r$:

$$f_r = \frac{1}{2\pi}\omega_r = \frac{1}{2\pi}\sqrt{\frac{s(x)}{m}} = \frac{1}{2\pi}\sqrt{\frac{\frac{s_0^s}{b\Delta X}e^{-\lambda x}}{\frac{m^s}{b\Delta X}}} = \frac{1}{2\pi}\sqrt{\frac{s_0^s e^{-\lambda x}}{m^s}} = \frac{1}{2\pi}\sqrt{\frac{s_0^s}{m^s}}e^{-\frac{\lambda x}{2}} \tag{3.27}$$

The damping is divided into a linear part $d_L(x)$ and a nonlinear part $d_N L(x)$. The linear part is based on $s(x)$ and for the nonlinear damping different choices exist. Remind from the mechanical oscillator the definition of the damping factor δ: $\delta = \frac{d}{\sqrt{ms}}$. With $s = s(x)$ from (3.26) and δ a given constant the damping becomes:

$$d(x) = d_L(x)d_{NL}(x) \text{ with } d_L(x) = \frac{\delta}{b\Delta X}\sqrt{m^s s^s(x)} = \frac{\delta}{b\Delta X}\sqrt{m^s s_0^s}e^{-\frac{\lambda x}{2}} \tag{3.28}$$

In the upcoming part, we choose to have linear damping, i.e. $d_{NL}(x) = 1$ but this simple choice is purely for the sake of research. The goal is to derive a new ME model and therefore the damping is kept simple.
We close the section by specifying the stimulus pressure p_e a bit more. Assume that we send a signal with one single frequency into the cochlea.

$$p_e = p_{AM1}\cos(2\pi f_1 t) \tag{3.29}$$

where p_{AM1} is the amplitude of the external stimulus, f_1 the frequency (Hz).

3.4 The electrical analagon of the 1D-model

Thus far we have derived a nice PDE for the 1D cochlea. From a mathematical point of view it would be a logic step to consult our theory in PDEs and find out if there exist nice solutions. However, in the upcoming section we will study an alternative way to deal with the cochlea through the electrical analagon. First, some basic theory in electrical engineering will be explained and applied afterwards to the model. This circuit model for the 1D cochlea is derived by van der Raadt in [4]. At the moment, the link between an electrical circuit and fluid dynamics seems quite far away but the similarity in describing the dynamics will hopefully be more clear afterwards.

3.4.1 Basic electronics

The basic knowledge in electronics will be illustrated by the RLC circuit in figure 3.5. The first two laws that hold in a circuit are the Kirchoff Current Law (KCL) and Kirchoff Voltage Law (KVL)

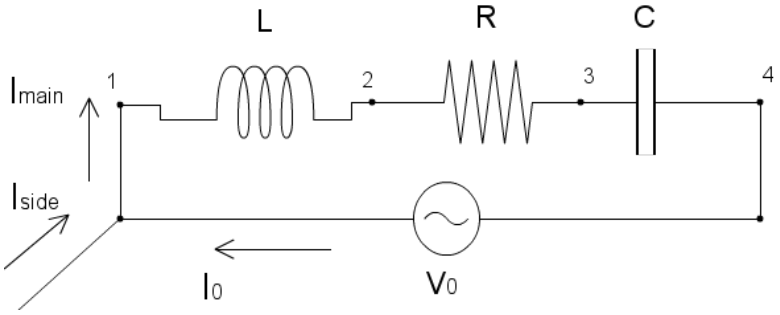

Figure 3.5: A basic RLC circuit with a side branche

- (KCL) In every node the sum of all in- and outcoming current is zero. So for example in the southwest node in the circuit of figure 3.5 this would give us: $I_0 + I_{side} - I_{main} = 0$.
- (KVL) In a closed loop the sum of all voltages is zero. A voltage is always measured between two points in the circuit, so in a closed loop both ends are at the same point. The KVL applied to figure 3.5 gives: $V_{1\to2} + V_{2\to3} + V_{3\to4} - V_0 = 0$.

The first element (between 1 and 2) is the inductor. An inductor resists changes in electric current passing through it. The voltage across the inductor is given by:

$$\Delta V(t) = L\frac{\partial I(t)}{\partial t} \tag{3.30}$$

with L the inductance. Keep in mind that I is a function of t since the power source gives an alternating current. Now we arrive at making an analagon of dynamics in electronics and mechanics. If we go back to (3.3) and transform this to an Euler equation for the volume flux q_v:

$$\frac{\partial p_v}{\partial x} = -\rho\frac{\partial u_v}{\partial t} = -\frac{\rho}{A_v}\frac{\partial q_v}{\partial t} \tag{3.31}$$

Compare (3.31) and (3.30) and we see the same dynamics. The x-derivative is the continuous version of the difference between sections and the pressure p resembles the voltage V. One can think of a voltage as the pressure which electrons are pushed through a wire. The volume flux q resembles the current I, think of the amount of electrons or the quantity of fluid that has to be transported per second. ρ represents a unit mass in the Euler equation, which is divided by a unit area. Hence, the inductance L represents the acoustic mass $m\left[\frac{kg}{m^4}\right]$ up to a minus sign that we should not forget.

The second element is the resistor which implements resistance in a circuit. The voltage is given:

$$\Delta V(t) = RI(t) \tag{3.32}$$

with R the resistance. Following the story of the inductor, this is equivalent with the linear damper in mechanics with $d\left[\frac{kg}{sm^4}\right]$ the acoustic damping:

$$\Delta p(t) = dq(t) \tag{3.33}$$

The third element is the capacitor which is able to store electrical charge. The voltage is given:

$$\Delta V(t) = \frac{1}{C}\int I(t)dt \tag{3.34}$$

With $s\left[\frac{kg}{m^4s^2}\right]$ the acoustic stiffness, this has the following equivalence in mechanics:

$$\Delta p(t) = s\int q(t)dt \tag{3.35}$$

If we combine the inductor, resistor and capacitor in series (as in the RLC circuit) we can add the voltages to form:

$$\Delta p(t) = m\frac{\partial q(t)}{\partial t} + dq(t) + s\int q(t)dt \tag{3.36}$$

We can now recognize the link of an RLC circuit with the mechanical oscillator of (3.10). Hence, an RLC circuit is also known as the electrical oscillator. The difference with (3.10) is the variable to solve which is now the flux $q\left[\frac{m^3}{s}\right]$ instead of the velocity $w\left[\frac{m}{s}\right]$. This is compensated by the acoustic mass, damping and stiffness which are defined per unit area. The displacement $y\,[m]$ is now the volume displacement indicated by $Y\left[m^3\right]$ and subsequently $q = \frac{\partial Y}{\partial t}$.

3.4.2 The circuit model of the cochlea

Now that we made the step from mechanics to electronics we can set up the circuit representing the 1D cochlea. Recalling figure 3.1 we have two compartments, the SV and ST, connected through the CP. As mentioned earlier, the hair cells are modeled as a row of operating oscillators on the CP, so for each section we have an RLC circuit in z-direction representing the motion of the cells on the CP. The CP connects the two chambers of fluid. The only mechanics in both chambers is the mass flow which is modeled with an inductor as explained above.
Connecting these elements gives the circuit given in the left panel of figure 3.6. The upper horizontal branche represents the mass flow of the cochlear fluid in the SV indicated by m_c by placing an inductor between each section.
Both chambers are connected by the electrical oscillator of section n, with mass m_n, damping d_n and stiffness s_n. For the left circuit of figure 3.6 the circuit equations are written out in the left column of Table 3.1.
To eliminate a part of the variables we derive a transformed sytem of circuit equations. By means of the local KCL's, we add the dynamics of the lower branches to the upper branch . To do this, we have to define a new variable:

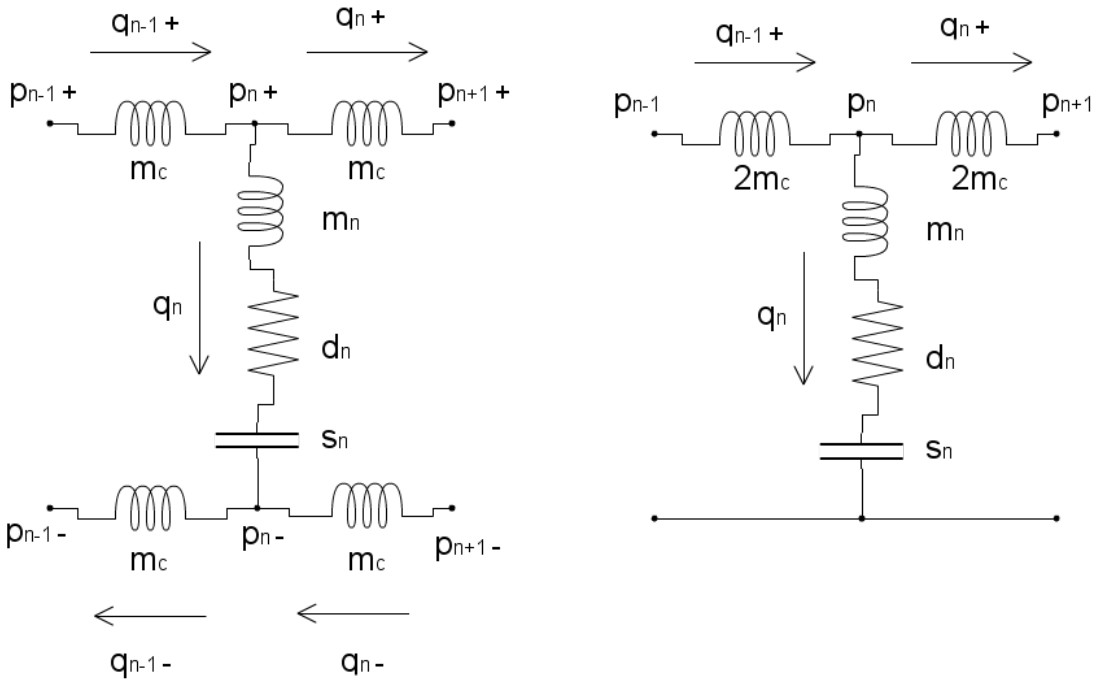

Figure 3.6: (left) The original circuit model for a single section in the cochlea; (right) the transformed circuit model for one cell.

$$p_n := p_n^+ - p_n^- \tag{3.37}$$

which results in the circuit in the right panel of figure 3.6 and the transformed equations in Table 3.1.

$$\begin{aligned} q_n &= q_{n-1}^- - q_n^- \\ m_c\tfrac{\partial q_n}{\partial t} &= m_c\tfrac{\partial q_{n-1}^-}{\partial t} - m_c\tfrac{q_n^-}{\partial t} \\ m_c\tfrac{\partial q_n}{\partial t} &= \left(p_n^- - p_{n-1}^-\right) - \left(p_{n+1}^- - p_n^-\right) \\ m_c\tfrac{\partial q_n}{\partial t} &= -p_{n-1}^- + 2p_n^- - p_{n+1}^- \end{aligned} \qquad \begin{aligned} q_n &= q_{n-1}^+ - q_n^+ \\ m_c\tfrac{\partial q_n}{\partial t} &= m_c\tfrac{q_{n-1}^+}{\partial t} - m_c\tfrac{q_n^+}{\partial t} \\ m_c\tfrac{\partial q_n}{\partial t} &= \left(p_{n-1}^+ - p_n^+\right) - \left(p_n^+ - p_{n+1}^+\right) \\ m_c\tfrac{\partial q_n}{\partial t} &= p_{n-1}^+ - 2p_n^+ + p_{n+1}^+ \end{aligned}$$

Original circuit	**Transformed circuit**
$p_{n-1}^+ - p_n^+ = m_c\frac{\partial q_{n-1}^+}{\partial t}$ $p_n^+ - p_{n+1}^+ = m_c\frac{\partial q_n^+}{\partial t}$ $q_{n-1}^+ = q_n + q_n^+$	$p_{n-1} - p_n = 2m_c\frac{\partial q_{n-1}^+}{\partial t}$ $p_n - p_{n+1} = 2m_c\frac{\partial q_n^+}{\partial t}$ $q_{n-1}^+ = q_n + q_n^+$
$p_n^- - p_n^+ = m_n\frac{\partial q_n}{\partial t} + d_n q_n + s_n\int q_n dt$	$p_n = m_n\frac{\partial q_n}{\partial t} + d_n q_n + s_n\int q_n dt$
$p_n^- - p_{n-1}^- = m_c\frac{\partial q_{n-1}^-}{\partial t}$ $p_{n+1}^- - p_n^- = m_c\frac{\partial q_n^-}{\partial t}$ $q_{n-1}^- = q_n + q_n^-$	

Table 3.1: The original circuit equations and the result of the transformation

Add both results for $m_c\frac{\partial q_n}{\partial t}$ and we will find:

$$\begin{aligned} 2m_c\frac{\partial q_n}{\partial t} &= \left(-p^-_{n-1} + 2p^-_n - p^-_{n+1}\right) + \left(p^+_{n-1} - 2p^+_n + p^+_{n+1}\right) \\ &= \left(p^+_n - p^-_{n-1}\right) - 2\left(p^+_{n-1} - p^-_n\right) + \left(p^+_{n+1} - p^-_{n+1}\right) := p_{n-1} - 2p_n + p_{n+1} \end{aligned}$$

If we transform the circuit to the circuit in the right panel of figure 3.6 we get an equivalent result:

$$\left.\begin{aligned} p_{n-1} - p_n &= 2m_c\frac{\partial q^+_{n-1}}{\partial t} \\ p_n - p_{n+1} &= 2m_c\frac{\partial q^+_n}{\partial t} \end{aligned}\right\} p_{n-1} - 2p_n + p_{n+1} = 2m_c\frac{\partial q^+_{n-1}}{\partial t} - 2m_c\frac{\partial q^+_n}{\partial t} = 2m_c\frac{\partial q_n}{\partial t} \quad (3.38)$$

From the vertical branche in figure 3.6 we have:

$$p_n = m_n\frac{\partial q_n}{\partial t} + d_n q_n + s_n\int q_n dt := m_n\frac{\partial q_n}{\partial t} + g_n \iff \frac{\partial q_n}{\partial t} = \frac{p_n - g_n}{m_n} \quad (3.39)$$

With this new definition of g_n, (3.38) becomes:

$$\boxed{p_{n-1} - 2\left(1 + \frac{m_c}{m_n}\right)p_n + p_{n+1} = -2\frac{m_c}{m_n}g_n} \quad (3.40)$$

This equation is boxed since it is important and we should keep it in mind.

The next step is to extend the model throughout the entire cochlea. To connect all the sections the circuit representing one cell is simply repeated. Eventually this would give us a system with N parallel oscillators connected through inductors. We only have to consider both ends of the cochlea. According to PDE theory we have to impose boundary conditions.

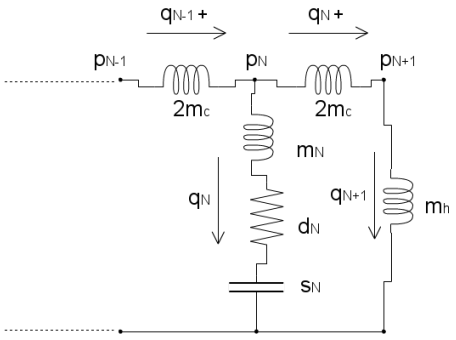

Figure 3.7: The circuit for the most right cell in the cochlea

Start with the helicotrema at $n = N$. In the anatomy of the cochlea we learned that this is the place where the CP ends and cochlear fluid is able to flow from SV to ST. Since we have N oscillators, at $n = N$ we will place the final oscillator and add a point at

$n = N + 1$ to model the mass flow through the helicotrema. This is done by an inductor with acoustic mass in the helicotrema m_h (details of m_h are specified later). This gives the circuit in Figure 3.7. The circuit equations for figure 3.7 can be written down at $n = N, N + 1$ and the same process is followed.

n=N	**n=N+1**
$q^+_{N-1} = q^+_N - q_N$	$q^+_N = q_{N+1}$
$p_{N-1} - p_N = 2m_c \frac{\partial q^+_{N-1}}{\partial t}$	$p_N - p_{N+1} = 2m_c \frac{\partial q^+_N}{\partial t}$
$p_N = m_N \frac{\partial q_N}{\partial t} + d_N q_N + s_N \int q_N dt$	$p_{N+1} = m_h \frac{\partial q_{N+1}}{\partial t}$

$$p_N - p_{N+1} = 2m_c \frac{\partial q^+_N}{\partial t} = 2m_c \frac{\partial q_N}{\partial t} = 2\frac{m_c}{m_h} m_h \frac{\partial q_{N+1}}{\partial t} = 2\frac{m_c}{m_h} p_{N+1} \tag{3.41}$$

$$\iff p_N = \left(1 + 2\frac{m_c}{m_h}\right) p_{N+1} \iff p_{N+1} = \left(\frac{m_h}{m_h + 2m_c}\right) p_N \tag{3.42}$$

$$2m_c \frac{\partial q_N}{\partial t} = p_{N-1} - 2p_N + p_{N+1} = p_{N-1} - \left(2 - \frac{m_h}{m_h + 2m_c}\right) p_N \tag{3.43}$$

$$\frac{\partial q_N}{\partial t} = \frac{p_N - g_N}{m_N} \iff 2m_c \frac{\partial q_N}{\partial t} = \frac{2m_c}{m_N} (p_N - g_N) \tag{3.44}$$

Combine (3.43) and (3.44) to get the final result:

$$p_{N-1} - \left(2 - \frac{m_h}{m_h + 2m_c} + \frac{2m_c}{m_N}\right) p_N = -2\frac{m_c}{m_N} g_N \tag{3.45}$$

$$\boxed{p_{N-1} - \left(1 + \frac{2m_c}{m_h + 2m_c} + \frac{2m_c}{m_N}\right) p_N = -2\frac{m_c}{m_N} g_N} \tag{3.46}$$

The ME was modeled by an oscillator with mass m_m, damping d_m and stiffness s_m. This gives the circuit of figure 3.8. Also, the stimulus is represented here by the voltage source $n_t p_e$, where the factor n_t comes from the transformator equation from (3.21).

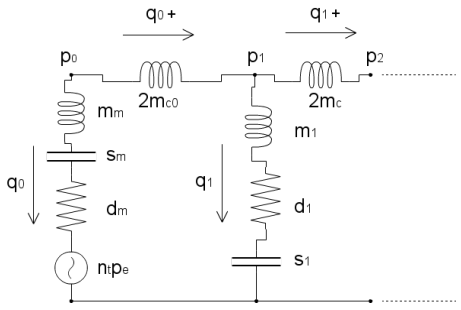

Figure 3.8: The circuit for the most left cell in the cochlea

With the following circuit equations:

n=0
$q_0 = -q_0^+$
$p_0 - p_1 = 2m_{c0}\frac{\partial q_0^+}{\partial t}$
$p_0 - n_t p_e = m_m \frac{\partial q_0}{\partial t} + d_m q_0 + s_m \int q_0 dt$

Define g_0 in the same way as for other values of n.

$$p_0 - p_1 = 2m_{c0}\frac{\partial q_0^+}{\partial t} = 2m_{c0}\left(\frac{n_t p_e - p_0 - g_0}{m_m}\right) \tag{3.47}$$

$$\boxed{-\left(1 + \frac{2m_{c0}}{m_m}\right)p_0 + p_1 = -\frac{2m_{c0}}{m_m}n_t p_e - \frac{2m_{c0}}{m_m}g_0} \tag{3.48}$$

Finally, combine all circuit parts to a circuit model for the total cochlea.

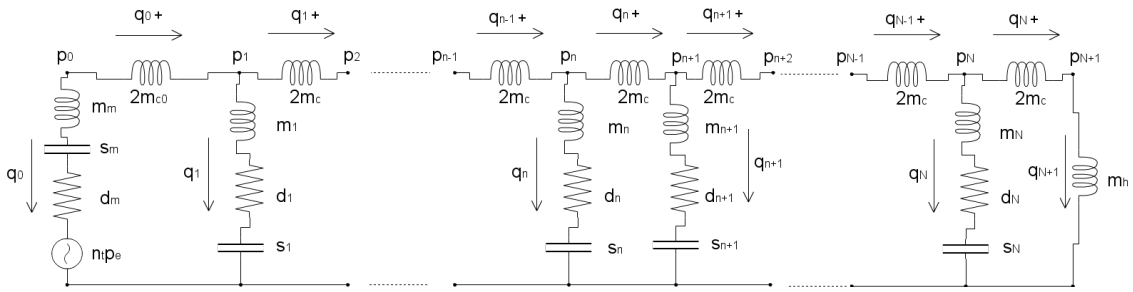

Figure 3.9: The circuit for the total cochlea

The equations derived above form the equations for the circuit model of the cochlea. These can be placed in a linear system:

$$A\mathbf{p} = \mathbf{r} \tag{3.49}$$

Where A is an $N+1$ - by - $N+1$ matrix with the coefficients for $\mathbf{p}$ a vector of size $N+1$ and $\mathbf{r}$ the known right hand side with the same size as $\mathbf{p}$.

$$\begin{pmatrix} a_{11} & 1 & & & \\ 1 & a_{22} & 1 & & \\ & \ddots & \ddots & \ddots & \\ & & 1 & a_{N,N} & 1 \\ & & & 1 & a_{N+1,N+1} \end{pmatrix} \begin{pmatrix} p_0 \\ p_1 \\ \vdots \\ p_{N-1} \\ p_N \end{pmatrix} = \begin{pmatrix} r_0 n_t p_e - r_0 g_0 \\ r_1 g_1 \\ \vdots \\ r_{N-1} g_{N-1} \\ r_N g_N \end{pmatrix} \tag{3.50}$$

$$
\begin{aligned}
a_{11} &= -\left(1+\frac{2m_{c0}}{m_m}\right) \\
a_{nn} &= -2\left(1+\frac{2m_c}{m}\right), n \in 2,\ldots,N \\
a_{N+1,N+1} &= -\left(1+\frac{2m_c}{m_h+2m_c}+\frac{2m_c}{m}\right) \\
r_0 &= -\frac{2m_{c0}}{m_m} \\
r_n &= -\frac{2m_c}{m}, n \in 2,\ldots,N+1
\end{aligned}
$$

We see that A has the tridiagonal $[1 \quad -2 \quad 1]$ - structure at each row which is the finite difference approximation matrix, call it L_2. This corresponds with the $\frac{\partial^2}{\partial x^2}$-term in (3.15). It is supplemented with the mass terms coming from the vertcial branches.

Solving (3.49) will give us a solution for $\mathbf{p}$ through the cochlea. We may have to ask ourselves whether it is always possible to solve this system, i.e. is A nonsingular? To show this we use the concept of a diagonal dominant matrix.

Definition 1 *A diagonally dominant matrix is a matrix A with the property $|a_{ii}| \geq \sum_{j\neq i}|a_{ij}|$ for all i. When these inequalities are strict, the matrix is called strictly diagonally dominant.*

□

By checking all the rows of A we can show that A is a diagonal dominant matrix.

$$
\begin{aligned}
|a_{11}| &= |-\left(1+\frac{2m_{c0}}{m_m}\right)| = |\left(1+\frac{2m_{c0}}{m_m}\right)| > 1 = |a_{12}| \\
|a_{nn}| &= |-2\left(1+\frac{2m_c}{m}\right)| > 2 = 1+1 = |a_{n,n-1}|+|a_{n,n+1}|,\ n \in 2,\ldots,N \\
|a_{N+1,N+1}| &= |-\left(1+\frac{2m_c}{m_h+2m_c}+\frac{2m_c}{m}\right)| > 1 = |a_{N+1,N}|
\end{aligned}
$$

For diagonal dominant matrices we can use Lemma 1.

Lemma 1 *A is a diagonally dominant matrix $\Longrightarrow$ A is nonsingular.*

□

The conclusion is that we do not have to worry about any inconvenience with A being singular. We will not focus further on solution methods for (3.49) but just use a standard routine like Gauss elimination.

We continue with our process to find a solution for the displacement y of the CP. First

of all, this is done solving for the volume displacement $Y[m^3]$. The displacement $y[m]$ is then calculated by dividing through the surface on which the volume displaces ($b\Delta X$or $A_v = bh$ depending on the direction).

Assume that at a time stage $t^{(j)}$ we have:

$$\begin{aligned}\mathbf{q}^{(j)} &= \left[q_0^{(j)}, q_1^{(j)}, \ldots, q_{N-1}^{(j)}, q_N^{(j)}\right] \\ \mathbf{Y}^{(j)} &= \left[Y_0^{(j)}, Y_1^{(j)}, \ldots, Y_{N-1}^{(j)}, Y_N^{(j)}\right]\end{aligned} \tag{3.51}$$

We calculate $\mathbf{g}^{(j)}$ rather easily:

$$\mathbf{g}^{(j)} = d\mathbf{q}^{(j)} + s\mathbf{Y}^{(j)} \tag{3.52}$$

Then solve the linear system of (3.49) to find:

$$\mathbf{p}^{(j)} = \left[p_0^{(j)}, p_1^{(j)}, \ldots, p_{N-1}^{(j)}, p_N^{(j)}\right] \tag{3.53}$$

From this result we want to reach the new time stage $t^{(j+1)}$. This is done by using equation (3.39):

$$\frac{\partial q_n}{\partial t} = \frac{p_n - g_n}{m_n} \tag{3.54}$$

And for the equation to go from the flux q to displacement Y:

$$q_i = \frac{\partial Y_i}{\partial t} \tag{3.55}$$

Equation (3.55) holds for all $i \in 0, 1, \ldots, N$. The same for (3.54) with an exception for $i = 0$:

$$\frac{\partial q_0}{\partial t} = \frac{p_0 - n_t p_e - g_0}{m_m} \tag{3.56}$$

(3.54), (3.55) and (3.56) can be solved with an explicit time integration method. One of the most accurate methods would be a fourth order Runge Kutta time integration which gives us a solution for $q^{(j+1)}$ and $Y^{(j+1)}$. Runge Kutta requires to execute the process of solving (3.49) four times per timestep. In between these four steps, estimates for $q^{(j+1)}$ and $Y^{(j+1)}$ are used and weighted to get a very accurate solution. For simplicity, we use a standard explicit time integration, the explicit Euler method. The results can be used to calculate $g^{(j+1)}$ and we can just repeat the process we started at (3.51).

3.5 Overview

To give some structure in the equations of the one-dimensional model and the process of solving a small overview is necessary. Define M, D and S are diagonal matrices with the value for m_i, d_i and s_i at every postion x_i and $c = \frac{2\rho}{h}$. L_2 is the tridiagonal matrix representing the finite difference approximation of the second order derivative, for the structure see (3.50). At time stage $t^{(n)} = n\Delta t$ we want to solve $\mathbf{Y}^{(n)} = [Y_0^{(n)}, Y_1^{(n)}, \ldots, Y_N^{(n)}]$.

The PDE of (3.14) becomes:

$$L_2\left(M\ddot{\mathbf{Y}} + D\dot{\mathbf{Y}} + S\mathbf{Y}\right) - cI\ddot{\mathbf{Y}} = 0 \tag{3.57}$$

Write (3.55) and (3.52) as:

$$\begin{aligned} \dot{\mathbf{Y}}(t) &= \mathbf{q}(t) && (3.58)\\ \mathbf{g}(\mathbf{q}, \mathbf{Y}) &= D\mathbf{q} + S\mathbf{Y} && (3.59) \end{aligned}$$

such that (3.57) becomes:

$$L_2\left(M\dot{\mathbf{q}} + \mathbf{g}(\mathbf{q}, \mathbf{Y})\right) - cI\dot{\mathbf{q}} = 0 \tag{3.60}$$

Next we have $\mathbf{p}$ from (3.36) and find an explicit formula for $\dot{\mathbf{q}}$:

$$\mathbf{p}(t) = M\dot{\mathbf{q}}(t) + \mathbf{g} \Longleftrightarrow M\dot{\mathbf{q}} = \mathbf{p} - \mathbf{g} \Longleftrightarrow \dot{\mathbf{q}} = M^{-1}(\mathbf{p} - \mathbf{g}) \tag{3.61}$$

Substitution of (3.61) in (3.60) results into the linear system:

$$\left(L_2 - cM^{-1}\right)\mathbf{p} = cM^{-1}\mathbf{g} \tag{3.62}$$

The system of (3.62) must be solved for $\mathbf{p}$ accompanied by the ODE's given by (3.58) and (3.61). The process of solving these equations in time is given stepwise.

Step 1: Calculate the right hand side $\mathbf{g}$ through (3.59): $\mathbf{g}^{(n)} = d\mathbf{q}^{(n)} + s\mathbf{Y}^{(n)}$.
Step 2: Solve (3.62): $A\mathbf{p}^{(n)} = cM^{-1}\mathbf{g}^{(n)} \longmapsto \mathbf{p}^{(n)}$, with $A = L_2 - cM^{-1}$. The dense matrix structure is presented in more detail below ($r_i = cm_i^{-1}$).

$$\begin{pmatrix} a_{11} & 1 & & & \\ 1 & a_{22} & 1 & & \\ & \ddots & \ddots & \ddots & \\ & & 1 & a_{N,N} & 1 \\ & & & 1 & a_{N+1,N+1} \end{pmatrix} \cdot \begin{pmatrix} p_0 \\ p_1 \\ \vdots \\ p_{N-1} \\ p_N \end{pmatrix} = \begin{pmatrix} r_0 n_t p_e - r_0 g_0 \\ r_1 g_1 \\ \vdots \\ r_{N-1} g_{N-1} \\ r_N g_N \end{pmatrix} \tag{3.63}$$

Step 3: Solve (3.61): $\dot{\mathbf{q}} = \frac{\mathbf{p}^{(n)} - g^{(n)}}{m} \longmapsto \mathbf{q}^{(n+1)}$ by applying an explicit time integration.
Step 4: Solve (3.58): $\dot{\mathbf{Y}} = \mathbf{q}^{(n+1)} \longmapsto \mathbf{Y}^{(n+1)}$ again by applying an explicit time integration.

Repeat all steps with $n = n + 1$ until the last time step is reached. This gives us the total solution for Y at all points in time n and points in space i. A schematic overview of all the steps is given in figure 3.10.

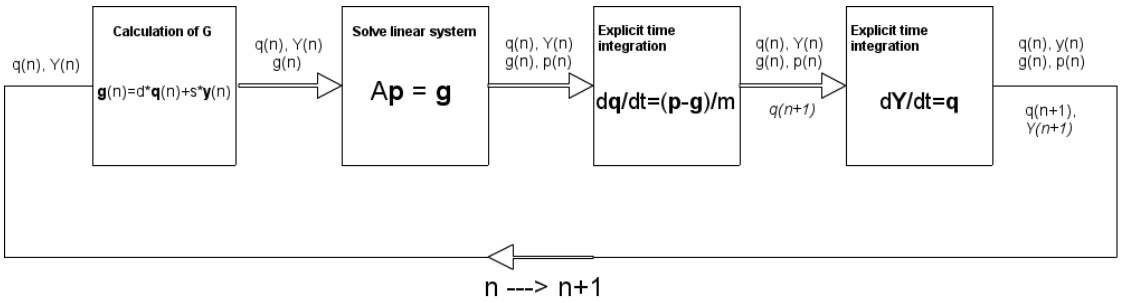

Figure 3.10: An overview of the process described in [4]

Chapter 4

Extension to the middle ear

In the past section the details of modeling the cochlea have become more clear. The aim of this thesis is to study the cochlea model and extend this model to the ME. In the previous section the cochlea model proposed by van der Raadt was studied in great detail and we will use this knowledge to derive a hopefully more accurate model for the ME. Up to this stage, the ME was represented as the far left oscillator in the cochlea. Mechanical influences of the ME were taken into account at this point in the model but we will study the ME in more detail to find out whether there is space for improvement. First, we will ask ourselves the question why the ME model should be improved. A proposed model by O'Connor and Puria [1] will be introduced and coupled to the cochlea. We will see that the ME model resembles the cochlea model in many ways. However, some difference in mechanics will lead to a problem in the equations. A solution and an adjusted model for both the ME and the cochlea will be presented.

4.1 Why study and improve the model for the ME?

If we consider the anatomy of the cochlea we can see that a stimulus always passes the ME. It is remarkable that in the cochlea model of figure 3.9 the ME is represented by a single oscillator while it anatomically consist of three ossicles. These ossicles are connected but are individually able to move with their own dynamics and have their own effect on the stimulus. It is well known that the main function of the ME is to efficiently transfer the acoustic energy from air to fluid to make the dynamics suitable for analysis in the cochlea [8]. The apparent complex anatomy and functions of the ME versus the simple interpretation in the cochlea model so far indicates that there is some space for improvement:

- Which elements form the ME and what is the function of these elements? We have to find out whether these elements can be represented by the single oscillator element and whether it is wise to expand the element structure.

- Is it possible to translate the ME elements to the circuit model interpretation as presented by [4] ?

- Can this circuit model be coupled to the cochlea model and be solved?

An improved ME model could give more explanation to problems audiologists encounter. Basically, a better understanding and implementation of the ME model would contribute to the development in the previously mentioned applications in audiological research and engineering.

4.2 Physiology of the ME and O'Connor and Puria's circuit model

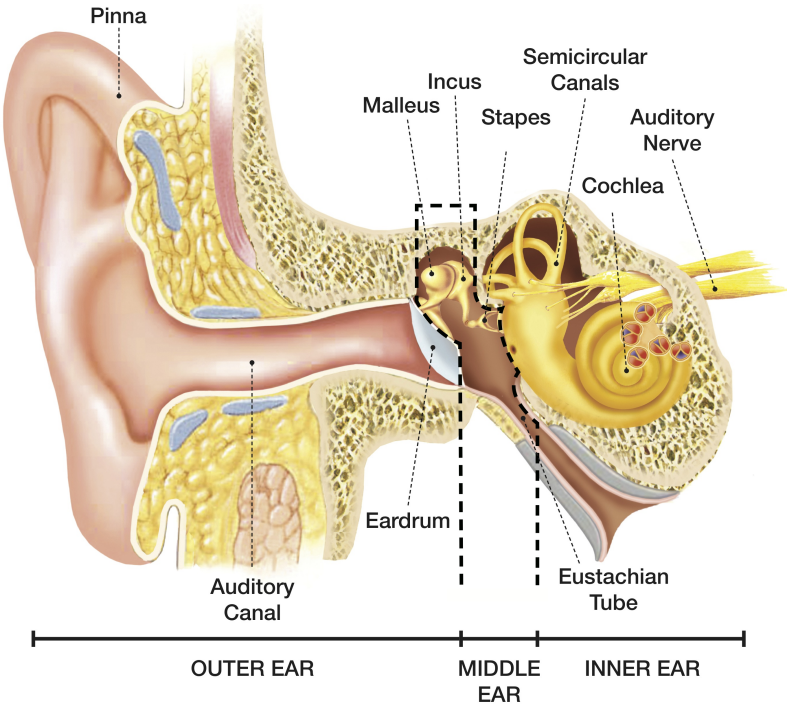

Figure 4.1: The physiology of the ear

The model for the ME starts by taking a closer look at the physiology of the ME. Therefore, consider figure 4.1 specifically for the ME. We will walk through the process of a stimulus entering the ear from the outside world and slowly work towards a circuit model proposed by O'Connor and Purina in [1]. The are many other proposals for the ME model but our choice for this model is based on the fact that this is published quite recently and uses the right mix of simplifications of the problem and amount of elements that are important to consider. Moreover, it uses the same the circuit formulation as the one-dimensional circuit model for the cochlea.

- A stimulus enters the outer ear and passes through the ear canal to arrive at the ear drum. As mentioned earlier, the effects of the ear canal are neglected.

- The outer ear and ME are separated by the tympanic membrane (TM) , or ear drum. The stimulus meets an acoustic impedance Z_{ec} and this impedance is transformed to Z_{oc} when it passes the TM. The physics behind the TM will be worked out later.

- The transformed stimulus enters the ME which consists of the ME cavity and three ossicles called the ossicular chain. The effects of the ME cavity are incorporated in the paramters of the TM. This simplifies the fitting procedure and once the TM block is characterized, it is possible to produce an approximate full middle-ear model by later adding suitable ME cavity model [1]. The three ossicles are called the malleus, incus and stapes and operate as three mechanical levers to transfer the sound energy through the ME to the oval window, the entrance to the cochlea. The ossicles are attached to the walls of the ME cavity through ligaments. Furthermore, the incudo-malleolar joint (IM joint) connects malleus with incus and the incudostapedial joint connects the incus with the stapes (IS joint).

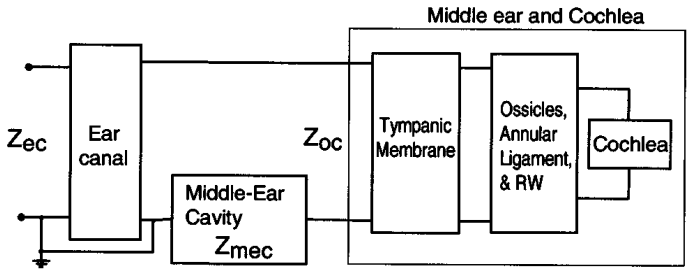

Figure 4.2: Schematic overview of the ME by Puria and Allen in [7]

A schematic overview of the ear is given in figure 4.2. No technical details are given yet but this figure gives a nice indication how the circuit model for the ME will look like. We will now write out the ME model in equations. The described processes are all mechanical but to remain consistent with the acoustic variables in the cochlea model we transform to acoustic equations.

Tympanic membrane

The TM converts the vibrations in the air that come from the left side to vibrations in the malleus, the connected ossicle at the right hand side of the TM. This conversion means that the incoming acoustic impedance $Z_{tm} = \frac{p_{tm}}{q_{tm}}$ is mapped to a new impedance going into the malleus $Z_{oc} = \frac{p_{mal}}{q_{mal}}$. In the circuit this is modeled by a so called acoustic transmission line. A transmission line is a model for the transfer of energy through a medium. During transportation, properties in the medium like velocity and pressure can change. In terms of impedance we say that it maps a source impedance Z_{tm} to a load impedance Z_{oc} by a process called *impedance matching*. When this matching is not ideal, a part of the load signal will not be transmitted but reflected by the line. This is quantified by a reflection coefficient [7]:

$$R(\omega) = |R(\omega)|e^{i\phi(R(\omega))} = \frac{Z_{tm}(\omega) - Z_{oc}(\omega)}{Z_{tm}(\omega) + Z_{oc}(\omega)} \tag{4.1}$$

The first equality sign of (4.1) is the decomposition of the reflection in amplitude and phase indicating that the transmission not only effects the amplitude but also the phase of the load signal. This is called the *delay* of the transmission line. The circuit model of

[1] is not very explicit about the elements contained in the transmission line and keeps this as a two-port block system. However, [7] is one of the few articles that does make a choice which we will use (and probably is used in [1]). The transmission line is modeled as a mass m_{tm} with a shunt stiffness s_{tm}, see figure 4.3.

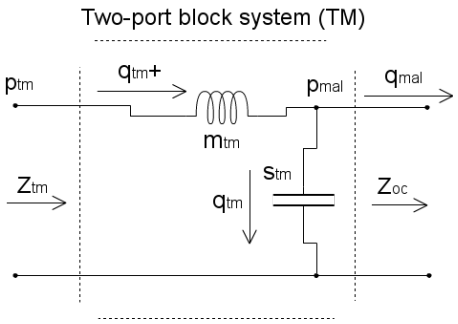

Figure 4.3: The two-port block system of the TM including the circuit elements

Malleus
The malleus itself is an ossicle which has a mass and is able to rotate. Mass is displaced through rotation so therefore we define the mass m_{mal} and this can be modeled in the same way as mass flow in the cochlear fluid, i.e. with an inductor. The value of m_{mal} can be calculated from:

$$m_{mal} = \frac{m^w_{mal}\kappa^2}{L^2_{mal}} \tag{4.2}$$

where m^w_{mal} is the measured mass, κ the radius of gyration and L_{mal} the length of the malleus. Dividing by the square of the area where the mass is acting, the area of the TM A_{tm} gives the acoustic mass (unit $\frac{kg}{m^4}$). This holds for all parameters in the ME.
The ligament connecting the malleus and the incus with the walls of the ME cavity contains damping and stiffness represented by d_{mal} and s_{mal} respectively.

Incus and IM/IS-joint
The incus is also an ossicle capable to rotate which is modeled with an inductor of mass m_{inc}. The ligament connecting incus with the wall is taken into account in d_{mal} and s_{mal}. The incus is both connected with the malleus and stapes through the IM and IS joint respectively. These connecting elements both contain damping and stiffness represented by d_{IM}, s_{IM}, d_{IS} and s_{IS} but no mass term.

Stapes and the OW/RW
The stapes itself is a moving ossicle with mass m_{sta}. The connection at the left is already modeled in the IS joint. At the right it has a connection through a so called annular ligament with the OW. This is the position where sound energy will be transferred through the OW on its way to the cochlea. The annular ligament has damping and stiffness d_{sta} and s_{sta}. In the cochlea model it was assumed that the influences of the OW are incorporated in the ME, this assumption still holds and we assume its stiffness is in the value of s_{sta}. For the RW this assumption was more doubtful and therefore we assume it has a stiffness s_{RW} which should be placed at the lower half of the circuit.

However, by applying the same transformation as been done for the mass m_c in the ST in section 3, we can place the capacitor with s_{RW} in the upper branche next to the stapes.

Take all elements specified in previous paragraphs and the circuit model for the cochlea derived in previous section in figure 3.9. Until now, the ME was represented by a single oscillator at $n = 0$. It is now time to extend the cochlea model with the ME model from O'Connor and Puria [1]. We remove the oscillator at $n = 0$ and couple the cochlea model in the same way as indicated by figure 4.2. The resulting circuit model is given in figure 4.4.

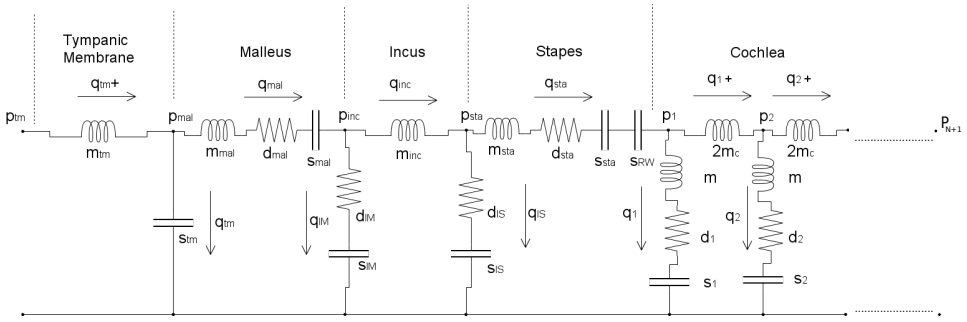

Figure 4.4: The circuit model for the ME coupled to the cochlea

4.3 Extension of the circuit equations

The circuit modeling phase of the ME is done and it is now time to work out the circuit equations for the ME part in exactly the same way as for the cochlea. Before doing that, let us observe the coupled cochela and ME model in figure 4.4 and spot some differences on the circuit branches between the cochlea part and the ME part.

- On the upper horizontal branches not only inductors but also resistors and capacitors are placed. Furthermore, in the TM there is a delay element which is not studied yet and a resistor takes place instead of an inductor.
- On the vertical branches representing the IM and IS joint the inductor is missing.

These differences in elements are justified since the physiology of the ME is simply different. Let us consider a point in the ME, say p_{sta}, and just work out the equations as we did in section 3.4.2 to study the consequences.

$$q_{inc} = q_{sta} + q_{IS} \tag{4.3}$$

$$p_{sta} - p_1 = m_{sta}\frac{\partial q_{sta}}{\partial t} + d_{sta}q_{sta} + (s_{sta} + s_{RW})\int q_{sta}dt := m_{sta}\frac{\partial q_{sta}}{\partial t} + g_{sta} \tag{4.4}$$

$$p_{inc} - p_{sta} = m_{inc}\frac{\partial q_{inc}}{\partial t} \tag{4.5}$$

$$p_{sta} = d_{IS}q_{IS} + s_{IS}\int q_{IS}dt := g_{IS} \tag{4.6}$$

The next step was to add the two upper branches:

$$p_{inc} - 2p_{sta} + p_1 = m_{inc}\frac{\partial q_{inc}}{\partial t} - m_{sta}\frac{\partial q_{sta}}{\partial t} - g_{sta} \tag{4.7}$$

The two differentials were added by differentiating the KCL of (4.4). However, the term $\frac{\partial q_{sta}}{\partial t}$ has a prefactor m_{sta} and $\frac{\partial q_{inc}}{\partial t}$ the prefactor m_{inc}. In the cochlea these two differentials could be added since all masses were identically $2m_c$. We could overcome this problem by doing the following modification.

$$\begin{aligned} m_{inc}\frac{\partial q_{inc}}{\partial t} + m_{sta}\frac{\partial q_{sta}}{\partial t} &= m_{inc}\frac{\partial q_{inc}}{\partial t} + m_{inc}\frac{\partial q_{sta}}{\partial t} - m_{inc}\frac{\partial q_{sta}}{\partial t} + m_{sta}\frac{\partial q_{sta}}{\partial t} \\ &= m_{inc}\frac{\partial q_{IS}}{\partial t} + (m_{sta} + m_{inc})\frac{\partial q_{sta}}{\partial t} \end{aligned}$$

The term $\frac{\partial q_{sta}}{\partial t}$ could be substituted back by rewriting (4.4):

$$p_{sta} - p_1 = m_{sta}\frac{\partial q_{sta}}{\partial t} + g_{sta} \Longrightarrow \frac{\partial q_{sta}}{\partial t} = \frac{p_{sta} - p_1 - g_{sta}}{m_{sta}} \tag{4.8}$$

BUT! This is not possible for the branche of the IS joint in (4.6) since it does not contain a term $\frac{\partial q_{IS}}{\partial t}$. The KCL incorporates the vertical branche through the derivatives of q but since there is no mass term anymore this is impossible. If we would try to write (4.4) in the same form as (4.4) we would have to divide by m_{IS} which is zero. The same problem would emerge in the IM joint and the TM where the shunt masses are absent.

A possible solution is to artificially add mass terms in the equations in the ME to overcome this problem of a zero mass. The disadvantage is that the model may not represent the ME as well as the original model would do. Moreover, these masses should stay very close to zero to give an accurate model which will lead to elements in the system approaching infinity. Tweaking the other parameters could compensate this but later on, the parameters should also be tweaked to fit experimental data. These data contain a lot of features like the reaction on different frequencies and amplitudes. Also there are a lot of choices to be made in damping and stiffness (we saw this in section 3). We can imagine that this is a very complex process and entering this process with already constraints concerning artificial parameters is not desirable.

***Conclusion**: The ME model of O'Connor and Puria could be coupled to the cochlea model of van der Raadt but it is impossible to solve the circuit equations in the same way as van der Raadt described for the cochlea. The reason is the difference in physiology between the cochlea the ME.*

4.4 The implicit cochlea model

So how are we going to deal with this technical problem? Is there a method to solve the ME circuit model without redefining the model? In the upcoming section we present the answer to this questions.

Start with considering the KVL of a random branche from p_i to a neighbouring p_j in the circuit model of figure 4.4 containing all the possible combinations electrical elements.

$$p_j - p_i = m_{ij}\frac{\partial q_{ij}}{\partial t} + d_{ij}q_{ij} + s_{ij}\int q_{ij}dt \tag{4.9}$$

We discretize in time by assigning mesh size dt and grid points $t^{(n)} = n \cdot dt$ and performing an implicit time discretization:

$$p_j^{(n+1)} - p_i^{(n+1)} = m_{ij}\left(\frac{q_{ij}^{(n+1)} - q_{ij}^{(n)}}{dt}\right) + d_{ij}q_{ij}^{(n+1)} + s_{ij}\int q_{ij}^{(n+1)}dt \tag{4.10}$$

$$q = \frac{\partial Y}{\partial t} \Longrightarrow Y^{(n+1)} = Y^{(n)} + dtq^{(n+1)} \tag{4.11}$$

For the integral term in (4.9) this means:

$$\int q_{ij}^{(n+1)}dt = \int q_{ij}^{(n)}dt + q_{ij}^{(n+1)}dt = Y_{ij}^{(n)} + q_{ij}^{(n+1)}dt \tag{4.12}$$

Combine the results of (4.10) and (4.12) to solve for $q_{ij}^{(n+1)}$:

$$p_j^{(n+1)} - p_i^{(n+1)} = m_{ij}\left(\frac{q_{ij}^{(n+1)} - q_{ij}^{(n)}}{dt}\right) + d_{ij}q_{ij}^{(n+1)} + s_{ij}\left(Y_{ij}^{(n)} + q_{ij}^{(n+1)}dt\right) \tag{4.13}$$

$$\Rightarrow \quad \left(p_j^{(n+1)} - p_i^{(n+1)}\right)dt = \left(m_{ij} + d_{ij}dt + s_{ij}dt^2\right)q_{ij}^{(n+1)} - m_{ij}q_{ij}^{(n)} + s_{ij}Y_{ij}^{(n)}dt = 0$$

$$\Rightarrow \quad q_{ij}^{(n+1)} = \frac{m_{ij}}{m_{ij} + d_{ij}dt + s_{ij}dt^2}q_{ij}^{(n)} + \frac{dt}{m_{ij} + d_{ij}dt + s_{ij}dt^2}\left(p_j^{(n+1)} - p_i^{(n+1)}\right) - \frac{s_{ij}dt}{m_{ij} + d_{ij}dt + s_{ij}dt^2}Y_{ij}^{(n)} \tag{4.14}$$

The implicit version of the KCL is just:

$$\sum_{\text{all neighbouring j}} q_{ij}^{(n+1)} = 0 \tag{4.15}$$

Substitute the result of (4.14) in (4.15), take for example the point $i = 2$ in the cochlea:

$$\begin{cases} q_2^{+(n+1)} = q_2^{+(n)} + \frac{dt}{2m_c}(p_2^{(n+1)} - p_3^{(n+1)}) \\ q_1^{+(n+1)} = q_1^{+(n)} + \frac{dt}{2m_c}(p_1^{(n+1)} - p_2^{(n+1)}) \\ q_2^{(n+1)} = \frac{m}{(m_2+d_2dt+s_2dt^2)}q_2^{(n)} + \frac{dt}{(m_2+d_2dt+s_2dt^2)}p_2^{(n+1)} - \frac{s_2dt}{m_2+d_2dt+s_2dt^2}Y_2^{(n)} \end{cases}$$

The KCL at the top node of $i = 2$ is: $q_1^{+(n+1)} - q_2^{+(n+1)} - q_2^{(n+1)} = 0$.

$$\boxed{\begin{aligned} &-\frac{dt}{2m_c}p_1^{(n+1)} + \left(\frac{dt}{m_c} + \frac{dt}{m_2 + d_2dt + s_2dt^2}\right)p_2^{(n+1)} - \frac{dt}{2m_c}p_3^{(n+1)} = \\ &q_1^{+(n)} - \left(\frac{m}{m + d_2dt + s_2dt^2}\right)q_2^{(n)} - q_2^{+(n)} + \frac{s_2dt}{m + d_2dt + s_2dt^2}Y_2^{(n)} \end{aligned}} \tag{4.16}$$

This result provides the solution for the problem of the missing mass term! Equation (4.16) forms one equation in a linear system with solution p. It is the equivalent of equation (3.40) in section 3 but now formulated in an implicit way. The denominators of the system elements now consist of all present elements of the branche instead of only the mass. This has the big advantage that in the case of a $m = 0$ no problems emerge from dividing by zero. Except for the case that m, d and s all equal zero, but this is a nonrelevant case since we would not have any dynamics left. The circuit equations (3.46) and (3.48) for the helicotrema and the middle ear are also derived in implicit form.

The helicotrema ($i = N$):

$$\boxed{\begin{aligned} &-\frac{dt}{2m_c}p_{N-1}^{(n+1)} + \left(\frac{dt}{2m_c} + \frac{dt}{2m_c + m_h} + \frac{dt}{m_N + d_Ndt + s_Ndt^2}\right)p_N^{(n+1)} = \\ &q_{N-1}^{+(n)} - \left(\frac{m^s}{m_N + d_Ndt + s_Ndt^2}\right)q_N^{(n)} + \frac{s_Ndt}{m_N + d_Ndt + s_Ndt^2}Y_N^{(n)} \end{aligned}} \tag{4.17}$$

The ME ($i = 0$):

$$\boxed{\begin{aligned} &\left(\frac{dt}{2m_{c0}} + \frac{dt}{m_m + d_mdt + s_mdt^2}\right)p_0^{(n+1)} - \frac{dt}{2m_{c0}}p_1^{(n+1)} = \\ &-q_m^{+(n)} - \left(\frac{m_m}{m_m + d_mdt + s_mdt^2}\right)q_m^{(n)} + \frac{s_mdt}{m_m + d_mdt + s_mdt^2}Y_0^{(n)} + \frac{n_tm^sdt}{m_m + d_mdt + s_mdt^2}p_e^{(n)} \end{aligned}} \tag{4.18}$$

So we found the solution to our problem of a zero mass but this means we have to derive the whole cochlea and ME model in an implicit form. We could propose to do the cochlea in the original, explicit way since this already exists and the ME implicit since this is the area where zero masses occur. The problem is that the two models are connected with each other and solving these in a different order in time would lead to contradictions at the position where they connect. Therefore, it is logical to reformulate the cochlea model in implicit form. When this is done, we will extend the model with the new ME.
We return to the original circuit model for the cochlea in figure 4.5. First, to make things more clear, we will use a system formulation by contracting all variables into column vectors. Considering figure 4.5 we need to solve for $N+1$ points of p and $2\cdot(N+1) = 2N+2$ points of q. The branch at the helicotrema is merged with the branch of p_N to p_{N+1} so

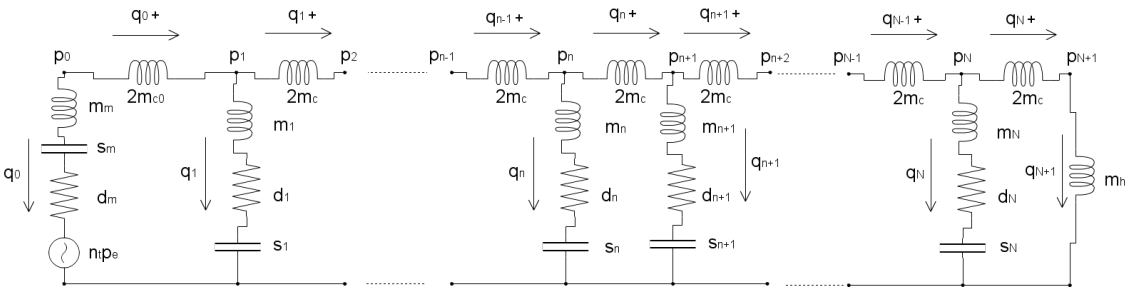

Figure 4.5: The circuit for the total cochlea

we consider one branche with two masses and we do not need to solve for p_{N+1} (this has also been done in the explicit cochlea model). Define the following vectors:

$$\mathbf{q}^{(n)} = \left[q_0^{(n)}, q_0^{+(n)}, q_1^{(n)}, q_1^{+(n)} \ldots, q_N^{(n)}, q_N^{+(n)}\right] \in \mathbb{R}^{2N+2}$$
$$\mathbf{Y}^{(n)} = \left[Y_0^{(n)}, Y_0^{+(n)}, Y_1^{(n)}, Y_1^{+(n)} \ldots, Y_N^{(n)}, Y_N^{+(n)}\right] \in \mathbb{R}^{2N+2}$$
$$\mathbf{p}^{(n)} = \left[p_0^{(n)}, p_1^{(n)}, \ldots, p_{N-1}^{(n)}, p_N^{(n)}\right] \in \mathbb{R}^{N+1}$$

Details concerning size and elements of all upcoming matrices and vectors will be given in the Appendix. For now, only the main structure of the system is relevant. (4.14) can now be written

$$\mathbf{q}^{(n+1)} = \tilde{M}^{-1}M\mathbf{q}^{(n)} + dt\tilde{M}^{-1}K^T\mathbf{p}^{(n+1)} - \tilde{M}^{-1}S\mathbf{Y}^{(n)} - dt\tilde{M}^{-1}K^T\mathbf{e}^{(n)} \tag{4.19}$$

where M, D, and S are define as diagonal matrices with elements m_i, d_i and s_i from (4.14) respectively. $\tilde{M}$ is the diagonal matrix with the elements $m_i + d_i dt + s_i dt^2$ which is non-singular. $\mathbf{e}^{(n)}$ represents the incoming stimulus; a row vector with the first element representing $p_e^{(n)}$ and the rest zeros. In fact, this is the implementation of a boundary condition. We write the KCL of (4.15) in its discrete version:

$$K\mathbf{q}^{(n+1)} = 0 \tag{4.20}$$

The structure of K derived from (4.15):

$$K = \begin{pmatrix} -1 & 1 & 1 & & & & & & \\ & & -1 & 1 & 1 & & & & \\ & & & \ddots & \ddots & \ddots & & & \\ & & & & & -1 & 1 & 1 & \\ & & & & & & & -1 & 1 \end{pmatrix} \in \mathbb{R}^{(N+1)\cdot(2N+2)} \tag{4.21}$$

where we can see the analagon with fluid dynamics. Equation (4.19) is just the discretized version (implicit) of the Navier-Stokes equation in terms of a flux $\mathbf{q}$ and (4.20) where K is the discrete equivalent of a flux that is divergence free. Substitute (4.19) in (4.20):

$$-dtK\tilde{M}^{-1}K^T\mathbf{p}^{(n+1)} = K\tilde{M}^{-1}M\mathbf{q}^{(n)} - dtK\tilde{M}^{-1}S\mathbf{Y}^{(n)} - dt\tilde{M}^{-1}K^T\mathbf{e}^{(n)} \tag{4.22}$$

Equation (4.22) is the equivalent of (4.16) and in terms of fluid dynamics the Poisson equation in the pressure. For more background in terms from fluid dynamics (like Navier-Stokes, divergence and Poisson) we refer to [3].

The right hand side of (4.22) is known. It is split in terms for $\mathbf{q}$, $\mathbf{Y}$ and the known boundary condition. The system has to be solved for $\mathbf{p}^{(n+1)}$. The solution $\mathbf{p}^{(n+1)}$ is then substituted in (4.19) to find $\mathbf{q}^{(n+1)}$. The result, in turn, can be used as the new right hand side for (4.22) to calculate $\mathbf{p}^{(n+2)}$. Switching between these processes gives the total solution for $\mathbf{q}$ throughout the time interval. Additionally, the Y^{n+1} can be calculated through an implicit time integration of $q^{(n+1)}$:

$$\mathbf{Y}^{(n+1)} = \mathbf{Y}^{(n)} + dt\mathbf{q}^{(n+1)} \tag{4.23}$$

The inverse of $\left(K\tilde{M}^{-1}K^T\right)$ from (4.22) should be calculated and it can be proven that $K\tilde{M}^{-1}K^T$ is indeed non-singular. If we observe the matrix K in (4.21), the $N+1$ rows of K are obviously linear independent, all rows contain a non-zero element with zero's in the rest of this column (at elements $k_{i,2i}$ for $i \in [1, 2, \ldots, N+1]$). This means that the row space spanned by the row vectors of K has dimension $N+1$, i.e. $rank(K) = N+1$. Now use the following properties:

Property 1 *Let $A \in \mathbb{R}^{m\times n}$ and $B \in \mathbb{R}^{n\times k}$ with rank(B) = n then the following statements hold:*

1. *rank(A) = rank(A^T)*
2. *rank(AB) = rank(A)*

□

Property 2 *Let $A \in \mathbb{R}^{n\times n}$, then:*

A is non-singular $\iff$ rank(A) = n, i.e. A has full rank

□

So from the first statement of property 1, for $K^T \in \mathbb{R}^{(2N+2)\times(N+1)}$ it follows that $rank(K^T) = N+1$.

$\tilde{M} \in \mathbb{R}^{(2N+2)\times(2N+2)}$ is the diagonal matrix with elements $m_i + d_i dt + s_i dt^2$ for $i \in [1, 2, \ldots, 2N+2]$ which is non-singular since m_i, d_i and s_i are never zero at the same value for i. Hence, $\text{rank}(\tilde{M}^{-1}) = 2N+2$.

Now, by expanding the second statement of property 1 to a product of three matrices, we can determine that:

$$rank(K\tilde{M}^{-1}K^T) = rank(K\tilde{M}^{-1}) = rank(K) = N+1 \tag{4.24}$$

So $K\tilde{M}^{-1}K^T$ is of full rank and therefore by property 2 it is non-singular.

The solving process schematically can be summarized as follows:

Given an initial condition at some time stage n: $\mathbf{q}^{(n)}$ and $\mathbf{Y}^{(n)}$.
Step 1: Solve (4.22) which gives $\mathbf{p}^{(n+1)}$
Step 2: Use result from step 1 in (4.19), this gives $\mathbf{q}^{(n+1)}$
Step 3: Use result form step 2 in (4.23) to calculate $\mathbf{Y}^{(n+1)}$

Repeat the steps for $n = n + 1$ until the final time stage is reached. Schematically this is given in figure 4.6.

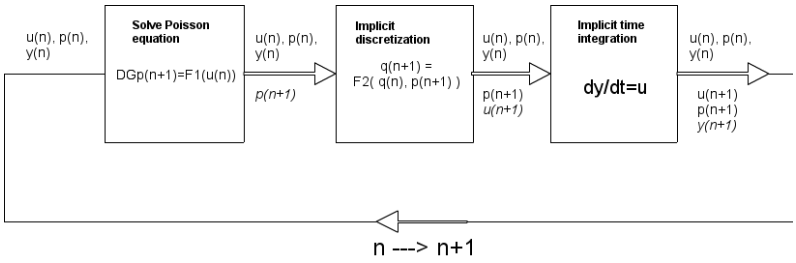

Figure 4.6: The schematic process for solving the implicit cochlea model

4.5 Differential algebraic equations

The choice for an implicit method for the cochlea is not only made because the equations work out pretty well. There is some more mathematical background behind this problem. Therefore, consider the KVL's once again (for simplicity the boundary condition $\mathbf{e}$ is left out and added later):

$$M\dot{\mathbf{q}}(t) = K^T\mathbf{p}(t) - \mathbf{g}(\mathbf{q}, \mathbf{y}) \tag{4.25}$$

$K^T : \mathbb{R}^{N+1} \longmapsto \mathbb{R}^{2N+2}$ maps $\mathbf{p}$ through the difference Δp to a KVL for every branche with flux $\mathbf{q}$, and it is the transpose of K which comes from the KCL:

$$K\mathbf{q}^{(n+1)} = 0 \tag{4.26}$$

which maps the fluxes $\mathbf{q}$ towards solutions for $\mathbf{p}$. Every timestep (4.25) and (4.26) are solved. This system is an example of a Differential Algebraic Equation (DAE). As the name suggests it is a system which contains both a differential part and an algebraic equation emerging from the singular part, this part is called the algebraic constraint. A more formal definition of a DAE is given by [10]:

Definition 2 *A Differential Algebraic Equation (DAE) system is a set of differential equations which can be expressed in general form as:*

$$F(t, \dot{\boldsymbol{q}}, \boldsymbol{q}, \boldsymbol{p}) = 0 \tag{4.27}$$

where $F : \mathbb{R}^{1+2n+m} \longmapsto \mathbb{R}^n$ *, F is singular (i.e. rank*$(\frac{\partial F}{\partial \boldsymbol{q}}) < n$*),* $\boldsymbol{u} \in \mathbb{R}^n$ *and* $\boldsymbol{p} \in \mathbb{R}^m$ *the input of the system.*

□

To see the connection of our problem with the definition write the system of (4.25) and (4.26) as:

$$F(t, \dot{\mathbf{q}}, \mathbf{q}, \mathbf{p}) = \begin{cases} F_1(t, \dot{\mathbf{q}}, \mathbf{q}, \mathbf{p}) & = -M\dot{\mathbf{q}}(t) - (\mathbf{p}(t) - \mathbf{g}(\mathbf{q}, \mathbf{y})) = 0 \\ F_2(t, \mathbf{q}) & = K\mathbf{q}^{(n+1)} = 0 \end{cases} \tag{4.28}$$

We can now see that the differential part is given by the KVL's and the algebraic part, which is often called the *constraint*, by the KCL. Actually, an ODE-system is a special case of a DAE where no algebraic part is present.
The system of (4.28) still has the secret assumption that M is non-singular. However, when the ME is incorporated some values of m may be zero leaving zero rows in M. So, M is becoming a singular matrix and some of the KVL's in (4.25) lose their dependence on $\dot{\mathbf{u}}$. In DAE theory this means these KVL's will become members of the algebraic part of the DAE. This means that initially the circuit model of the cochlea is a DAE-system with a nested DAE-system in the differential part showing itself when the ME is added to the cochlea.

So what is the difference between an ODE and a DAE in developing a solution method? The measure that defines the distance between a DAE and an ODE is given by the definition of an index [10].

Definition 3 *The differential index of a DAE system is the minimum number of times that all or part of the implicit differential equation of (4.27) must be differentiated with respect to t in order to determine $\dot{\boldsymbol{q}}$ as a continous function $\psi(t, \boldsymbol{q}, \boldsymbol{p})$.*

□

It is easily seen that an ODE has index 0 since the differential is already given explicitly $\dot{\mathbf{q}} = F(\mathbf{q}, \mathbf{p})$. The equations of motion of real time mechanical systems (as we are having in the cochlea model) often have index 3 or higher [9]. The index will not be worked out for the cochlea model, but the main message is finding a numerical method to solve these equations. Systems of higher order index often pose difficulties for applying numerical algorithms. A variety of problems such as robustness, error estimation and ill-conditioning emerge because of poorly conditioned constraints. However, these constraints are required by the physics and there are methods to reformulate DAE's to overcome these problems. An other problem is the *drift-off effect*; the numerical solution of the transformed systems tends to 'drift' away from the physical solution due to numerical errors in each timestep [9]. Solving DAE's and developing solution theory for the cochlea model would give a lot of research beyond the scope of this thesis and therefore we presented an alternative treatment for the problem by an implicit numerical method.
We head back to (4.25) and (4.26) and discard the definition of $\mathbf{g}$.

$$\begin{cases} M\dot{\mathbf{q}}(t) & = K^T\mathbf{p}(t) - D\mathbf{q}(t) - S\mathbf{y}(t) \\ K\mathbf{q}(t) & = 0 \end{cases} \tag{4.29}$$

This is still the case where M is non-singular. When we enter the ME equations M becomes singular and the algebraic part of the DAE system grows. The DAE system is now:

$$\begin{cases} \tilde{M}\dot{\mathbf{q}}(t) & = K_{ns}^T\mathbf{p}(t) - D_{ns}\mathbf{q}(t) - S_{ns}\mathbf{Y}(t) \\ 0 & = K_s^T\mathbf{p}(t) - D_s\mathbf{q}(t) - S_s\mathbf{Y}(t) \\ 0 & = K\mathbf{q} \end{cases} \tag{4.30}$$

The matrices indicated with subscript ns contain the non-singular part of the row equations and the singular (algebraic) part of the equations is separated from the differential part.

A growing singular part is disadvantageous for solving so we have chosen an alternative way. Consider the system of (4.29) again and discretize the time derivative implicitly giving:

$$\begin{aligned} M\frac{\mathbf{q}^{(n+1)} - \mathbf{q}^{(n)}}{dt} &= K^T\mathbf{p}^{(n+1)} - D\mathbf{q}^{(n+1)} - S\mathbf{Y}^{(n+1)} \\ &= K^T\mathbf{p}^{(n+1)} - D\mathbf{q}^{(n+1)} - S\left(\mathbf{Y}^{(n)} + dt\mathbf{q}^{(n+1)}\right) \\ \implies \left(M + dtD + dt^2S\right)\mathbf{q}^{(n+1)} &= M\mathbf{q}^{(n)} + dtK^T\mathbf{p}^{(n+1)} - dtS\mathbf{Y}^{(n)} \end{aligned}$$

We see that we overcome the problem of M being singular. The matrix to invert is now $M + dtD + dt^2S := \tilde{M}$ which allows us to have a singular M.

$$\mathbf{q}^{(n+1)} = \left(M + dtD + dt^2S\right)^{-1}\left(M\mathbf{q}^{(n)} + dtK^T\mathbf{p}^{(n+1)} - dtS\mathbf{Y}^{(n)}\right) \tag{4.31}$$

The result for $\mathbf{q}^{(n+1)}$ is also valid for the algebraic part of the DAE and would give:

$$\mathbf{q}^{(n+1)} = \left(dtD + dt^2S\right)^{-1}dtK^T\mathbf{p}^{(n+1)} - \left(dtD + dt^2S\right)^{-1}dtS\mathbf{Y}^{(n)} \tag{4.32}$$

Substitute (4.31) into the KVL of (4.30). This gives the linear system for $\mathbf{p}^{(n+1)}$:

$$-dtK\tilde{M}^{-1}K^T\mathbf{p}^{(n+1)} = K\tilde{M}^{-1}M\mathbf{q}^{(n)} - dtK\tilde{M}^{-1}S\mathbf{Y}^{(n)} \tag{4.33}$$

(4.33) and (4.31) are solved each timestep. The boundary condition $-dt\tilde{M}^{-1}K^T\mathbf{e}^{(n)}$ may be added to (4.31) and (4.33). So, by sliding forward the choice for an implicit time discretization solves the problem of singularity of M without applying theory for DAE's. This idea is inspired by the solution method for solving the Navier-Stokes equations for incompressible flow in CFD theory. The incompressiblity of fluid adds a constraint to the differential equations which is digested by applying the implicit time discretization before solving for $\mathbf{p}$. Eventually $\mathbf{p}$ is calculated by the Poisson equation which we can recognize in (4.33).

4.6 Results

The implicit cochlea model is implemented in Matlab, the code is provided in the Appendix. To validate the results of the implicit cochlea model we will run simulations and try to reproduce the results of the explicit cochlea model, from which the code is provided by INCAS^3.

For both time integrations, we offer a stimulus with frequency $f = 1000$ Hz, 60 dB amplitude during a time interval of 100 ms. First of all, we see that both models give a nice resonance at the characteristic position and damping through the rest of the cochlea. Also we see a significant difference in amplitude which we will discuss later this section. Through the frequency-place map (3.27) in section 3 and the parameters that can be found in the Appendix we can check whether the position of the resonance agrees with the frequency of the offered stimulus. Observe that we present the result x with the scaling $x = L\tilde{x}$, also in figure 4.7 to validate results with the INCAS^3 which is implemented with scaled variables.

$$f_r = \frac{1}{2\pi}\sqrt{\frac{s_0^s}{m^s}}e^{-\frac{\lambda\, x}{2}} \rightarrow 1000 = \frac{1}{2\pi}\sqrt{\frac{1*10^{10}}{0.5}}e^{-\frac{300*35*10^{-3}\tilde{x}}{2}} \rightarrow \tilde{x} = 0.59312 \tag{4.34}$$

which corresponds to the position of the maximum displacement in figure 4.7.

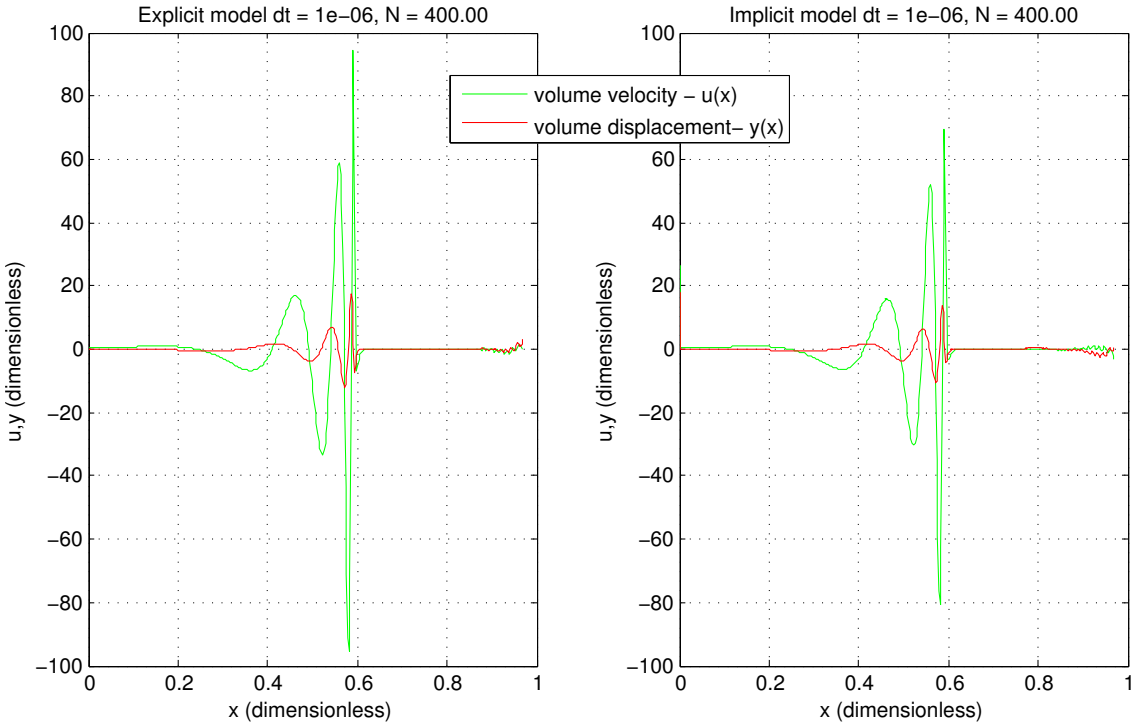

Figure 4.7: (Left) Solution for u and y in the explicit cochlea model. (Right) Solution for u and y in the implicit cochlea model.

First we discuss the choice for $N = 400$ and $dt = 10^{-6}$, as specified in Figure 4.7, which is not made randomly. There are some issues in the results that contaminate the robustness of both models. Research has been done and we observe the following:

- At the helicotrema ($\tilde{x} = 1$) we see small oscillations in the solution. When the grid is not fine enough the oscillations of the explicit solution tend to explode and as time marches onward the rest of the solution is dragged towards infinity. These oscillations also emerge in the implicit solution but stability is preserved for every choice of N. In future research one could possibly reconsider the modeling of the

boundary condition at the helicotrema. For now choose $N \geq 160$ to find stable solutions for both models.

- The same problem occurs when the timestep dt is not small enough. Again the oscillations drag the explicit solution towards infinity. Adapting N or the final time of the stimulus do not seem to solve this problem. It is recommended to choose $dt \leq 1.47 * 10^{-5}$ for stable solutions. This maximum value for dt corresponds with results of further stabiltity analysis at INCAS^3 [11]. The implicit method however, provides a stable solution for all choices of dt.

- From the previous two statements one may conclude that only the explicit method gives problems due to stability but there are other aspects. Indeed the implicit method provides stable solutions regardless the choice of dt and N, but it takes a small dt to have convergence of the implicit to the exact solution. The explicit time integration is a four step Runge Kutta integration which has fourth-order accuracy. Hence, the explicit solution is quite a good indication of how the exact solution will look like. In Figure 4.7, the choice $dt = 10^{-6}$ is made and we still see a significant difference in the amplitude of the explicit and implicit solution. Lowering dt would improve this result at the cost of computational effort. More on the difference in amplitude and the convergence of the method will be treated in the next section.

4.6.1 The amplitude envelope

To investigate the difference in amplitude at the resonance we provide plots of the so called analytic signal (not to confuse with the analytic solution) using the Hilbert transformation. Suppose we have a signal $x(t)$, the analytic signal is defined:

$$x_a(t) = x(t) + i\hat{x}(t) = x(t) + i\left(x(t) * \frac{1}{\pi t}\right) \tag{4.35}$$

where $\hat{x}(t)$ is the Hilbert transform. The Hilbert transform of a signal $x(t)$ is defined as the convolution with the function $\frac{1}{\pi t}$. The idea behind this transform is the following. If $x(t)$ is a real-valued signal then its Fourier spectrum $X(\omega) = \mathcal{F}(x(t))$ is symmetric around the zero-axis. Hence, we can discard the negative frequencies without loss of information of the signal. This is done by multiplying with the function Heaviside step function $u(\omega)$ and gives us the Fourier transform $X_a(\omega)$ of the analytic signal.

$$\begin{aligned} X_a(\omega) &= \begin{cases} 2X(\omega) & ,\omega > 0 \\ X(\omega) & ,\omega = 0 \\ 0 & ,\omega < 0 \end{cases} \\ &= X(\omega) \cdot 2u(\omega) = X(\omega) + X(\omega) \cdot sgn(\omega) \end{aligned}$$

Applying the inverse Fourier transform gives the analytic signal:

$$x_a(t) = \mathcal{F}^{-1}(X_a(\omega)) = \mathcal{F}^{-1}(X(\omega)) + \mathcal{F}^{-1}(X(\omega)) * \mathcal{F}^{-1}(sgn(\omega)) = x(t) + i\left(x(t) * \frac{1}{\pi t}\right) \tag{4.36}$$

The absolute value $|x_a(t)|$ of the analytic signal is called the *amplitude envelope* and gives a nice intuitive absolute plot of how the amplitude runs. It is now easier to analyze the absolute value of the amplitude for example two extreme values of a period who would first lie above and under the x-axis. The best way to see this is through an example plot given in figure 4.8.

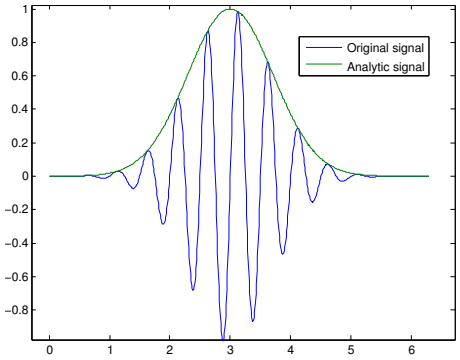

Figure 4.8: Example of signal and the corresponding analytical signal

We compute the analytical signals of the volume velocity u for both models which can be compared in figure 4.9. The Hilbert transform can be easily performed in Matlab through standard functions *hilbert* and *abs*.

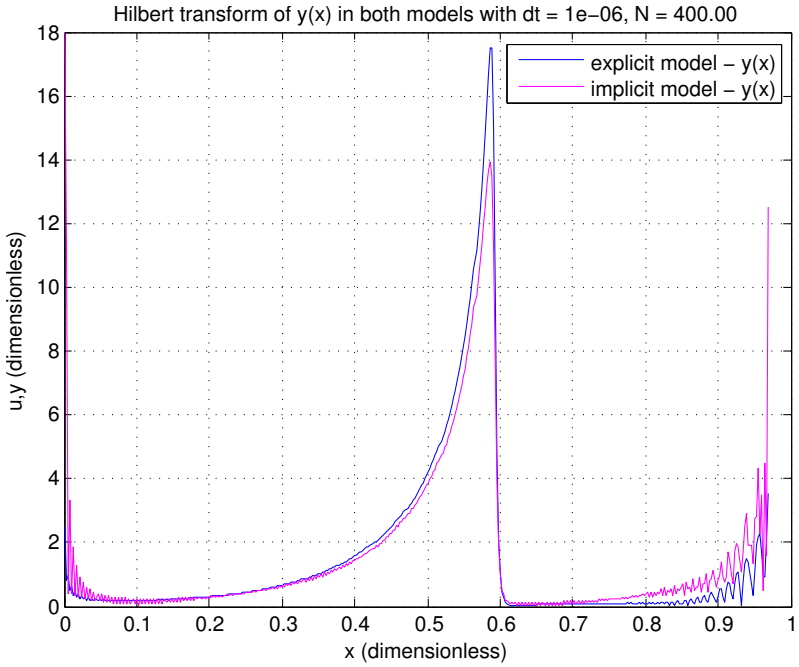

Figure 4.9: Absolute value of analytic solution $u_a(x)$ at $t = t_{end}$ for the explicit and implicit cochlea model

The analytic solution of both models seem to have the same shape and the difference in amplitude is also visible. As mentioned before, lowering dt would result in a better approximation of the solution of the explicit method. At the boundaries there are again

the problems of oscillations and exploding values. These events at the boundaries do not effect the important results at the resonance peak but are still an indication that boundary conditions should be reconsidered.

4.6.2 Artificial diffusion

An explanation for the difference in amplitude of the solution and the observation that lowering dt makes the solutions converge lies in the concept of artificial diffusion. We will illustrate this with the most simple PDE, the advection equation:

$$u_t + c \cdot u_x = 0 \tag{4.37}$$

Suppose we are looking for a solution u numerically and define a grid with cell width dx and dt in x-direction and time direction respectively. The Taylor expansions in the point (x_i, t_n)can be made:

$$u_i^{(n+1)} = u_i^{(n)} + dt \cdot u_t + \frac{1}{2} dt^2 \cdot u_{tt}$$
$$u_{i-1}^{(n)} = u_i^{(n)} - dx \cdot u_x + \frac{1}{2} dx^2 \cdot u_{xx}$$

Discretize (4.37) with the explicit Euler time discretization method and plug in the Taylor expansions. Some modifactions lead to:

$$u_t + c \cdot u_x = \frac{c}{2} dx \cdot u_{xx} - \frac{1}{2} dt \cdot u_{tt} = \frac{1}{2} c \left(1 - \frac{c \cdot dt}{dx}\right) dx \cdot u_{xx} \tag{4.38}$$

This new PDE is called the modified PDE of (4.37). It can now be seen that the discretization method actually describes the PDE in (4.38) and is only an approximation of (4.37). The modification is the right hand side which resulted from the explicit time discretization. It contains a term u_{xx} which is a diffusion term in PDE theory. The diffusion term is not in the original (natural) model but created by our numerical method (artificial) and is therefore called *artificial diffusion*. Reducing dx and dt will cause the modified PDE to converge to the original PDE.

We can do the same for the implicit Euler time discretization which leads to the following modified PDE:

$$u_t + c \cdot u_x = \frac{c}{2} dx \cdot u_{xx} + \frac{1}{2} dt \cdot u_{tt} = \frac{1}{2} c \left(1 + \frac{c \cdot dt}{dx}\right) dx \cdot u_{xx} \tag{4.39}$$

We see a comparable artificial diffusion with a plus instead of the minus sign in the explicit case. The difference in artificial diffusion between implicit and explicit method is:

$$\frac{1}{2} c \left(1 + \frac{c \cdot dt}{dx}\right) dx \cdot u_{xx} - \frac{1}{2} c \left(1 - \frac{c \cdot dt}{dx}\right) dx \cdot u_{xx} = cdx \cdot \frac{cdt}{dx} u_{xx} = c^2 dt \cdot u_{xx} \tag{4.40}$$

This result gives a possible explanation for the difference in amplitude of the solutions of the two cochlea models. The solutions are separated by the artificial diffusion term which depends on dt. An explanation for the observation that reducing dt results in

convergence of the implicit to the explicit method. Of course it has to be said that the PDE governing the cochlea model is much more complicated than the one in (4.37) but it gives a nice illustration. Moreover, there is an easier way in numerical analysis to prove the convergence of a method by Lax equivalence theorem.

Theorem 1 *(Lax equivalence theorem)*

For a consistent numerical method, zero-stability and convergence are equivalent.

□

A numerical method is consistent if the method has an order of accuracy $O(k^p)$ in a well-posed problem. The implicit Euler is known to have order of accuracy $O(k)$, so $p = 1$. Furthermore we assume that the problem is well-posed, i.e. it has correct boundary conditions and there exists a unique solution. For more formality and details on this topic we refer to [3]. The general idea of consistency is sufficient to understand the statements about convergence.

The last demand for convergence is the zero-stability of the method. Zero-stability means that if we have the following iteration process with iteration matrix A:

$$\mathbf{q}^{(n+1)} = A(dt)\mathbf{q}^{(n)} \tag{4.41}$$

on a finite time interval $[0, t_{end}]$ there exists a constant $K_{t_{end}}$ such that $\|A^n(dt)\| \leq K_{t_{end}}$ for $0 \leq n \leq \frac{t_{end}}{dt}$. In other words, the subsequent multiplication of A due to the iteration process on a finite time interval remains bounded. From [3] we have the following theorem:

Theorem 2 *When A is non-defect, we have the following equivalence property:*

The process of (4.41) is zero-stable $\Longleftrightarrow$ the spectral radius ρ of A satisfies the Von Neumann condition:

$$\rho(A) \leq 1 + O(dt) \tag{4.42}$$

where the order constant is independent of dt and dx.

□

We will show zero-stability using theorem 2. First we have to identify the iteration matrix A. The iteration process of the implicit cochlea model is recalled from (4.31):

$$\mathbf{q}^{(n+1)} = \left(M + dtD + dt^2S\right)^{-1}\left(M\mathbf{q}^{(n)} + dtK^T\mathbf{p}^{(n+1)} - dtS\mathbf{Y}^{(n)}\right) \tag{4.43}$$

We can find the iteration matrix by identifying the terms that connect $\mathbf{q}^{(n+1)}$ to $\mathbf{q}^{(n)}$ which is the matrix $\left(M + dtD + dt^2S\right)^{-1}M$. There are extra terms in $\mathbf{p}^{(n)}$ and $\mathbf{Y}^{(n)}$ which also depend on $\mathbf{q}^{(n)}$ through the Poisson equation (4.33) but these are $O(dt)$ in the Von Neumann condition of Theorem 2 due to the prefactor dt.

The iteration matrix $\left(M + dtD + dt^2S\right)^{-1}M$ is the diagonal matrix with diaognal elements $\frac{m_i}{m_i + d_i dt + s_i dt^2} \forall i \in [0, \ldots, N]$ as explained in section 4.4. The first demand is that

$\left(M + dtD + dt^2S\right)^{-1} M$ is non-defect which means that it is diagonalizable which is obviously satisfied since the matrix is diagonal. Now, the spectral radius of the iteration matrix can be calculated quite easily since the eigenvalues of a diagonal matrix are the diagonal elements itself:

$$\rho\left(\left(M + dtD + dt^2S\right)^{-1} M\right) = \max_i \left(\frac{m_i}{m_i + d_i dt + s_i dt^2}\right) \tag{4.44}$$

To estimate the last term of (4.44) we use the Taylor Series of the function $f(x) = \frac{1}{1+x}$ around $x = 0$:

$$f(x) = \frac{1}{1+x} \approx 1 - x + x^2 - x^3 + \ldots \Longrightarrow \frac{1}{1+x} \leq 1 - x + O(x^2) \tag{4.45}$$

And now use (4.45) to write:

$$\frac{m_i}{m_i + d_i dt + s_i dt^2} = \frac{1}{1 + \frac{d_i}{m_i} dt + \frac{s_i}{m_i} dt^2} \leq 1 - \left(\frac{d_i}{m_i} dt + \frac{s_i}{m_i} dt^2\right) + \text{h.o.t.} = 1 + O(dt) \tag{4.46}$$

So the results of (4.44) and (4.46) combined prove that the condition of (4.42) is satisfied. The $O(dt)$-terms in $\mathbf{p}^{(n)}$ and $\mathbf{Y}^{(n)}$ are added which does not change the result of (4.44) and according Theorem 2 zero-stability is satisfied. Finally, we apply Lax equivalence theorem to secure convergence of the implicit method of the cochlea model.

Chapter 5

The implicit middle ear model

The aim of the past sections in this thesis was the development of a more detailed model of the ME according to the circuit structure as in van der Raadt [4]. After we discovered restrictions in the middle ear which cause problems for the explicit cochlea model, it was decided to come up with an implicit version. Therefore, the last section was dedicated to deriving the implicit cochlea model and verification with the original model. Now it is time to use this basis for the development of an implicit ME model in the same model structure as for the cochlea. After the developement, its results will be verified with the results from O'Connor and Puria [1]. The ME will then be coupled to the cochlea. Some additional simulations with the total model will be done to identify the differences and opportunities with respect to the original model.

5.1 Circuit model and equations

The goal is to reproduce results presented by O'Connor and Puria. The original circuit model presented in this article is given in figure 5.1.

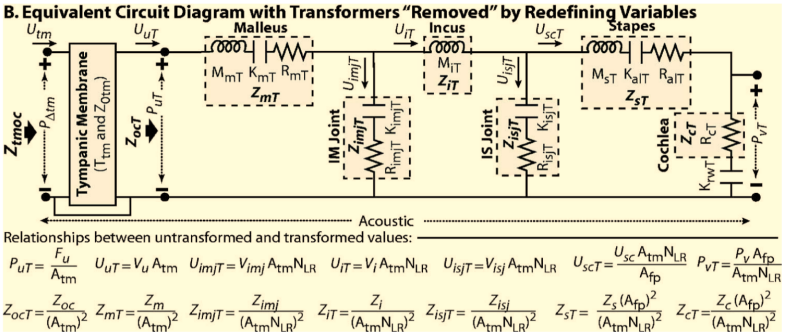

Figure 5.1: The ME model presented by O'Connor and Puria [1]

In the previous section we already explained some assumptions regarding the ME cavity and the implementation of the TM. Together with these assumptions we did the coupling with the cochlea and ended with the circuit model of figure 5.2 recalled from previous section. This is the ME model presented by O'Connor and Puria with a coupling to the cochlea model of van der Raadt. This is the form of the model we eventually desire, but

for the development of the implicit ME model we focus on the ME elements by replacing the cochlear part of the circuit with a resistor, see figure 5.3.

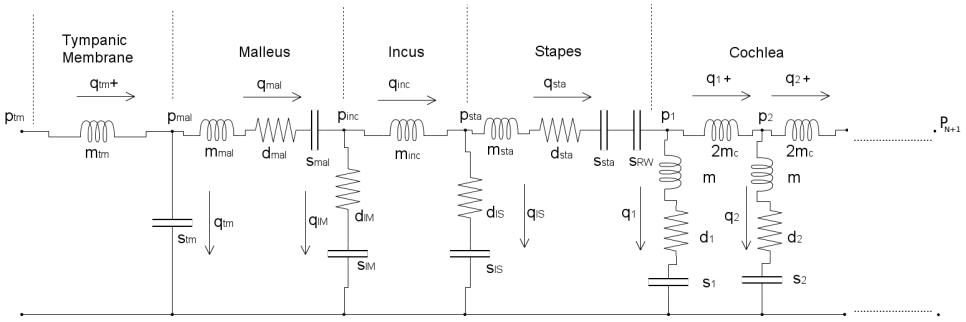

Figure 5.2: The circuit model for the ME coupled to the cochlea

The reason for this simplification is not only to allow ourselves to focus on the ME elements. It mainly has to do with the verification of our model with the model in figure 5.1. In this figure, the cochlear part is also represented with a resistor with a given damping value d_c so we copy this element. This adaption gives us the circuit model in figure 5.3.

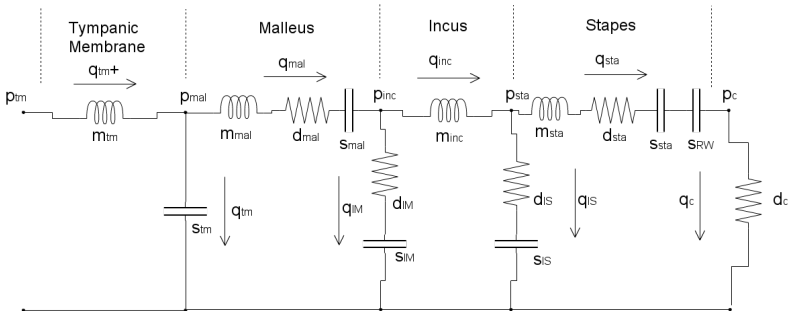

Figure 5.3: The circuit of the ME with simple cochlea

After verification, this implicit ME model is ready for coupling with the implicit cochlea model.

The circuit equations in the same matrix structure are now set up as presented in the previous section. Consider the circuit of figure 5.3. Applying the KCL gives the following equations:

$$\begin{cases} q_{tm}^{+} - q_{mal} - q_{tm} = 0 \\ q_{mal} - q_{inc} - q_{IM} = 0 \\ q_{inc} - q_{sta} - q_{IS} = 0 \\ q_{sta} = q_c \end{cases} \tag{5.1}$$

The KVL's of all the branches can be derived:

$$\begin{cases} p_{tm} - p_{mal} = m_{tm}\frac{\partial q_{tm}^{+}}{\partial t} \\ p_{mal} = s_{tm}\int q_{tm}dt \\ p_{mal} - p_{inc} = m_{mal}\frac{\partial q_{mal}}{\partial t} + d_{mal}q_{tm} + s_{mal}\int q_{mal}dt \\ p_{inc} = d_{IM}q_{IM} + s_{IM}\int q_{IM}dt \\ p_{inc} - p_{sta} = m_{inc}\frac{\partial q_{inc}}{\partial t} \\ p_{sta} = d_{IS}q_{IS} + s_{IS}\int q_{IS}dt \\ p_{sta} - p_c = m_{sta}\frac{\partial q_{sta}}{\partial t} + d_{sta}q_{sta} + (s_{sta} + s_{RW})\int q_{sta}dt \\ p_c = d_c q_c \end{cases} \tag{5.2}$$

After time discretization of the equations of (5.2) the result can be substituted in (5.1). An example of a row equation from the node located at the incus is given below:

$$\begin{aligned} &-\frac{dt}{m_{mal} + d_{mal}dt + s_{mal}dt^2}p_{mal}^{(n+1)} + \\ &\left(\frac{dt}{m_{mal} + d_{mal}dt + s_{mal}dt^2} + \frac{dt}{d_{IM}dt + s_{IM}dt^2} + \frac{dt}{m_{inc}}\right)p_{inc}^{(n+1)} - \frac{dt}{m_{inc}}p_{sta}^{(n+1)} \\ &= \frac{m_{mal}}{m_{mal} + d_{mal}dt + s_{mal}dt^2}q_{mal}^{(n)} - q_{inc}^{(n)} \\ &-\frac{s_{mal}dt}{m_{mal} + d_{mal}dt + s_{mal}dt^2}Y_{inc}^{(n)} + \frac{s_{IM}dt}{d_{IM}dt + s_{IM}dt^2}Y_{tm}^{(n)} \end{aligned} \tag{5.3}$$

The second fraction of the coefficient for p_{inc} in (5.3) does not show a mass. We see that the research and work done in the previous sections is now useful for the first time, a zero mass at the IM joint does not form a problem in the equations.

The matrix-vector structure is exactly the same as we saw for the implicit cochlea model. Only the elements and sizes of the matrices become different. For clarification, we present an overview of the equations.

$$\mathbf{q}^{(n+1)} = \tilde{M}^{-1}M\mathbf{q}^{(n)} + dt\tilde{M}^{-1}K^T\mathbf{p}^{(n+1)} - \tilde{M}^{-1}dtS\mathbf{Y}^{(n)} - dt\tilde{M}^{-1}K^T\mathbf{e}^{(n)} \tag{5.4}$$

$$-dtK\tilde{M}^{-1}K^T\mathbf{p}^{(n+1)} = K\tilde{M}^{-1}M\mathbf{q}^{(n)} - dtK\tilde{M}^{-1}S\mathbf{Y}^{(n)} - dt\tilde{M}^{-1}K^T\mathbf{e}^{(n)} \tag{5.5}$$

with

$$\begin{aligned} \mathbf{q}^{(n)} &= \left[q_{tm}^{+(n)}, q_{tm}^{+(n)}, q_{mal}^{(n)}, q_{IM}^{(n)}, q_{inc}^{(n)}, q_{IS}^{(n)}, q_{sta}^{(n)}, q_c^{(n)}\right] \in \mathbb{R}^8 \\ \mathbf{Y}^{(n)} &= \left[Y_{tm}^{+(n)}, Y_{tm}^{(n)}, Y_{mal}^{(n)}, Y_{IM}^{(n)}, Y_{inc}^{(n)}, Y_{IS}^{(n)}, Y_{sta}^{(n)}, Y_c^{(n)}\right] \in \mathbb{R}^8 \\ \mathbf{p}^{(n)} &= \left[p_{mal}^{(n)}, p_{inc}^{(n)}, p_{sta}^{(n)}, p_c^{(n)}\right] \in \mathbb{R}^4 \end{aligned}$$

and $\mathbf{e}^{(n)}$ representing $p_{tm}^{(n)}$, the pressure coming from a stimulus. The matrix K has the same structure as the matrix of (4.21) but with the size adapted for the ME, so $K \in \mathbb{R}^{4\times 8}$. The same for the matrices M, D and $S \in \mathbb{R}^{8\times 8}$ representing the mass, damping and stiffness elements in the ME. The equations are solved with the implicit method in Matlab. The relevant code can be found in the Appendix.

5.2 Results

The next step is to verify the results of the implicit ME model with the results from O'Connor and Puria. The results presented in this article can be found in figure 5.4. Based on measurement data of various sets of human middle ears all the parameters of the ME circuit are determined by a fitting procedure. More details of the measurements can be found in [1].

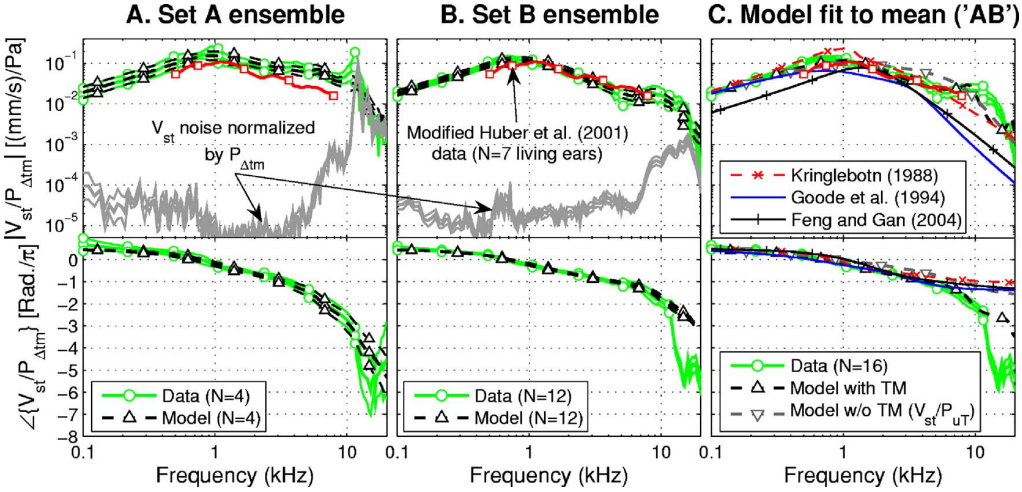

Figure 5.4: Model $\frac{u_{sta}}{P_{tm}}$ curves fitted through the data of measurements on different sets of human ears. Results from other methods in previous articles, reference in [1], are added and the cases with and without TM.

The plotted quantity is the ratio $\frac{u_{sta}}{p_{tm}}[\frac{mm/s}{Pa}]$. This specific ratio is chosen since u_{sta} is the velocity that enters the cochlear part of the model normalized by the pressure p_{tm} that entered the ME. Hence, the ratio of the two quantities is the transfer function in the frequency domain. Therefore the input and output signal $p_{tm}(t)$ and $u_{st}(t)$ respectively are Fourier transformed to $p_{tm}(\omega)$ and $u_{st}(\omega)$ by applying an FFT. The transfer of the input signal through the ME not only causes the amplitude to change but meanwhile a shift of the phase. It is plotted in units of $\frac{rad}{\pi}$, i.e. a phase shift of -2 is a shift of one whole period of a signal. The top three figures in figure 5.4 give the amplitude of $\frac{p_{tm}(\omega)}{u_{st}(\omega)}$ and the bottom three the phase. The frequency range is given $[0.1, 20]$ kHz, the hearing range of a healthy human ear, and is plotted with logarithmic scale.

The parameters that resulted from the fitting procedure can be found Table 1 of [1]. The values for data set C (the mean of the data of all human ears measured) are copied and used for the implicit model. The only parameters that were not explicitly mentioned

in [1] are the mass and stiffness of the TM. Since there is no further information about these parameters, we choose them to be in the same order of magnitude as the mass and stiffness of other elements in the ME resulting in $m_{tm} = 10^3 \frac{kg}{m^4}$ and $s_{tm} = 10^{12} \frac{kg}{s^2 m^4}$. To test the new model, this choice is sufficient. Later, these values could be tuned to fit experimental data.

The goal is to reproduce the results in figure 5.4 to verify the functionality of the new ME model. To get a smooth frequency spectrum of the transfer function we must have an input signal $p_{tm}(t)$ that contains every frequency within the specified range. There are two choices:

- *White Gaussian noise signal* A signal with a constant power spectral density over a certain bandwidth and uncorrelated for any pair in time. This means that the signal has equal power on every frequency within a specified frequency range and is completely random in each sense. In acoustics engineering, but also many other fields like statistical signal analysis, this type of signal is used. To give an idea how such a signal looks like, an example is presented in figure 5.5. The construction of this signal is done in Matlab through special packages for signal analysis.

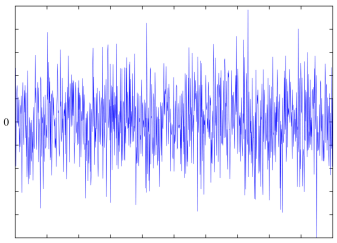

Figure 5.5: A white Gaussian noise signal

- *Delta function* A more simple, but more theoretical option is the delta function. It is defined as:

$$\delta(t) = \lim_{n\to\infty} r_n(t) \text{ with } r_n(t) = \begin{cases} n \text{ , if } |t| < \frac{1}{2n} \\ 0 \text{ , if } |t| > \frac{1}{2n} \end{cases} \tag{5.6}$$

  In audiology this is a rectangle of $\frac{1}{n}$ seconds and amplitude n at $t = 0$ and zero amplitude anywhere else. It has the important property that follows from the definition:

$$\int_{-\infty}^{\infty} \delta(t)dt = 1 \tag{5.7}$$

  Of course, physically seen there are problems with the limit $n \to \infty$. Producing a spike of zero seconds and infinite amplitude in practice is impossible. However, in many engineering applications the delta function is very useful and can be implemented in a discrete way just by a vector with zero elements and one element at an other value. The most interesting property for our topic is the Fourier transform of $\delta(t)$.

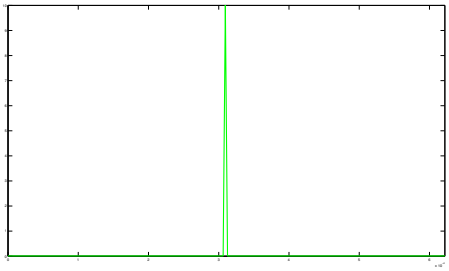

Figure 5.6: The delta function

$$\hat{\delta}(\omega) = \int_{-\infty}^{\infty} \delta(t) e^{-i\omega t} = 1 \tag{5.8}$$

Every frequency is contained in the spectrum of the delta function in equal power. In discrete sense, a time series with only zeros and one element a large value would be an acceptable approximation of the delta function and moreover it is very easy to implement. Therefore it is chosen as the input signal $p_{tm}(t)$ for the rest of the section.

We send the input signal $p_{tm}(t)$ through the implicit ME model and provide the same plots as in figure 5.4. Before analysis we have to consider an important factor which is the sample frequency. When solving the model equations in a discrete way, the time grid is divided in cells of length dt. Every dt seconds a new value of the input signal is presented and the solution is calculated. All dynamics that take place on a time scale smaller than dt are invisible. In terms of signal analysis, the waves with frequency higher that $f = \frac{1}{dt}$ are filtered out of the solution. f is the highest detectable frequency and is called the sample frequency. We need to detect the frequencies in the audible range, so at least frequencies up to 20 kHz should be detected. However, we set the sampling frequency at 40 kHz to prevent the phenomenon *aliasing*. The explanation of this phenomenon is done by considering figure 5.7. When sampling, it could happen that two signals of different frequencies have the same value in time as can be seen in the figure. Therefore, we are not able to distinguish these two frequencies. To prevent this, at first the sampling frequency must be high enough to detect the frequencies of interest (the same conclusion a few sentences ago). Moreover, to be able to see every 'bump' in the signal every half of a period must be detected increasing the sufficient sample frequency with a factor two. Half of the sample frequency is called the *Nyquist frequency*. Since an alias frequency is not distinguished from the real frequency the spectrum of the transfer function is the same for these frequencies. The alias frequency lies at the other side of the Nyquist frequency so the spectrum is symmetric around this point.
Now take a look at the results for the sampling frequencies 40 kHz and 320 kHz found in figure 5.8 (the reason for a second sample frequency is explained later). The amplitude at 40 kHz seems to fit the data in figure 5.4 quite nicely. A maximum transfer approximately in the middle of the audible range and decreasing when it reaches the boundaries. Only at the highest frequency the slope seems to tend to zero where the data indicate an ongoing descent. The reason for this is the symmetry of the frequency spectrum at the

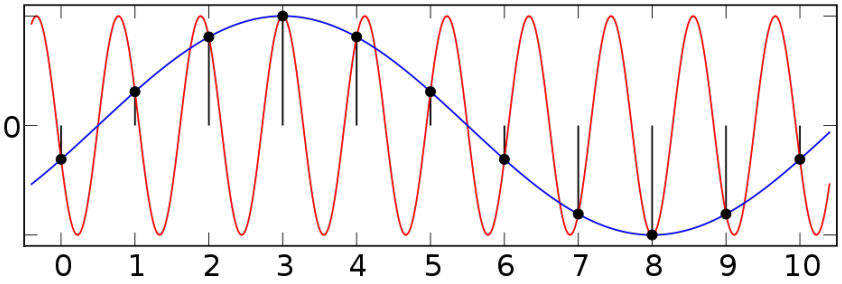

Figure 5.7: An example of the phenomenon 'aliasing' in signal analysis.

Nyquist frequency. The phase plot is somewhat less positive. At lower frequencies, the line is descending as the data of figure 5.4 demand. However, at higher frequencies this descent stops and the phase returns to zero shift at the Nyquist frequency. The reason for this feature is the value of the sample frequency. The sampling creates a time series of data every dt in time. It will automatically recognize a signal perfectly in phase with this data serie. In other words, the sample is in perfect alignment with itself. To prevent the zero slope in the amplitude and zero phase at 20 kHz, we have to increase the sampling frequency at the cost of simulation time. In signal analysis, it is common to perform sampling on a frequency a few factors higher than the region of interest.

Therefore in the implicit ME model, the sampling frequency is set to 320 kHz which resulted in the right plots of figure 5.8. We see that the zero slope has disappeared in the amplitude which fits the data better. The phase shows better descent at high frequencies since the Nyquist frequency has been shifted to the right. Still, the minimum is visible which indicates the phase wil return to zero at 320 kHz. This could be solved by increasing the sampling frequency much more. In [1] the used sample frequency is not given.
More material for comparison is available by plotting other transfer functions in the ME model. In figure 5.9, amplitude and phase plots of three other transfer functions are compared with measurements from [1]. These transfer functions are calculated in the implicit ME model as well. Results are presented in figure 5.10.
Again, there is a good agreement of the results of our implicit model with the data provided in figure 5.9. We can conclude that we have an ME model rewritten in implicit form which shows results similar to models presented in the literature.

5.3 Adding the cochlea to the ME

The cochlea in the model from the previous section (figure 5.1) was kept simple. We have presented some nice results when solving this ME model implicitly which provided validation with results of [1]. It is time to couple this ME model to the cochlea model and solve the total ear model implicitly. The associated circuit model was already given in the previous section in figure 5.2. So the difference between the models is the cochlear part where we had the *simple cochlea* represented by a single resistor d_c and the new total ear model where the cochlear part is the *cochlea model* described in 3. The equations of both model are implemented in Matlab (for the code, see the Appendix). To illustrate

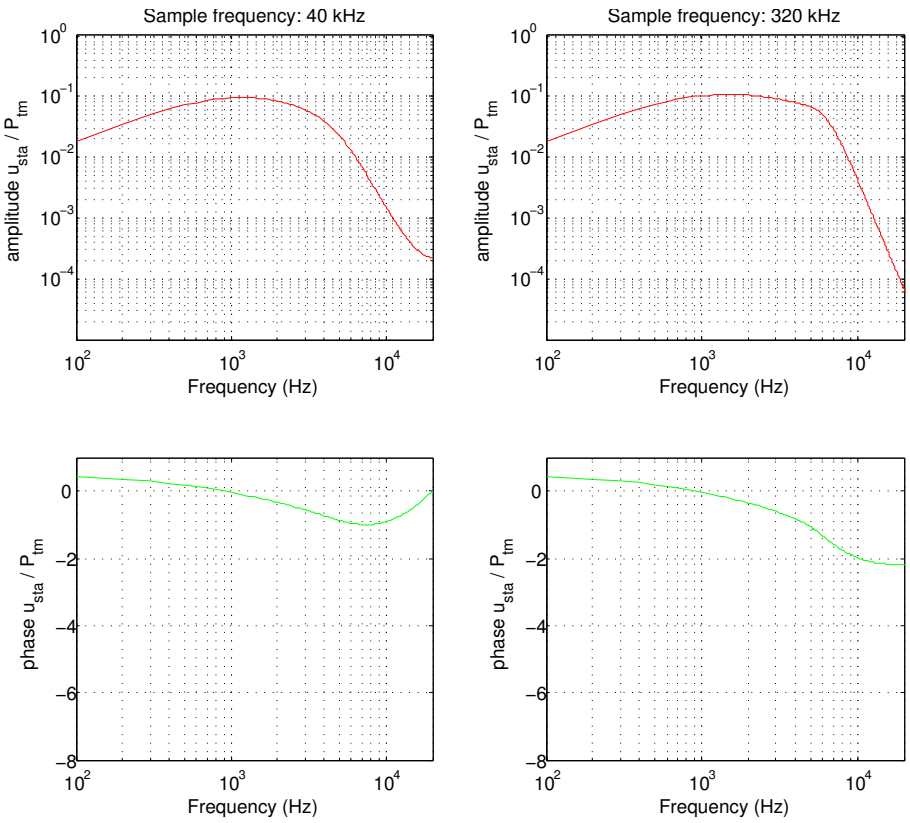

Figure 5.8: Amplitude and phase plots of the transfer function $\frac{u_{sta}}{P_{tm}}$ of the implicit ME model for two different sample frequencies.

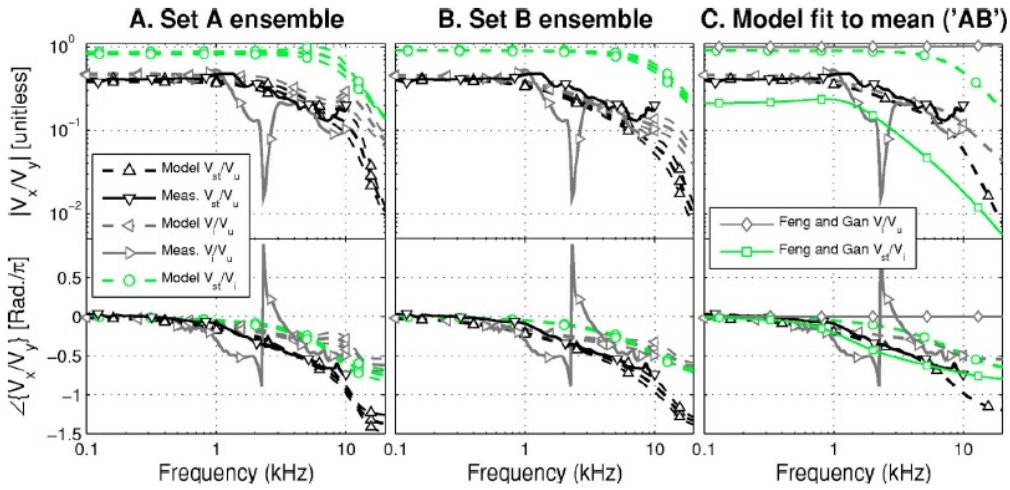

Figure 5.9: Model curves from three other transfer functions in the ME compared with measurement data. u_{mal}, u_{inc} and u_{sta} have notation V_u, V_i and V_{st} respectively

the consequences of coupling the cochlea model, the same transfer plots are made for this model and compared to the version with the simple cochlea in figure 5.11.

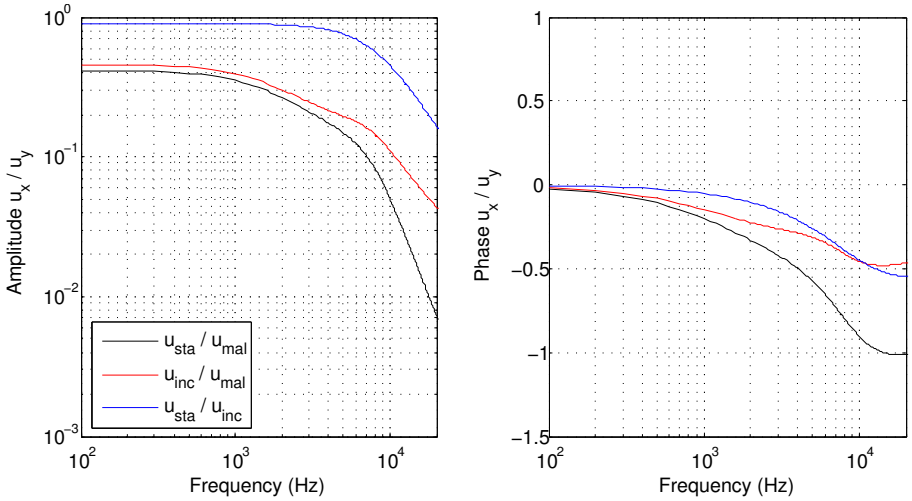

Figure 5.10: Amplitude and phase plots of three transfer functions in the implicit ME model at a sample frequency of 320 kHz.

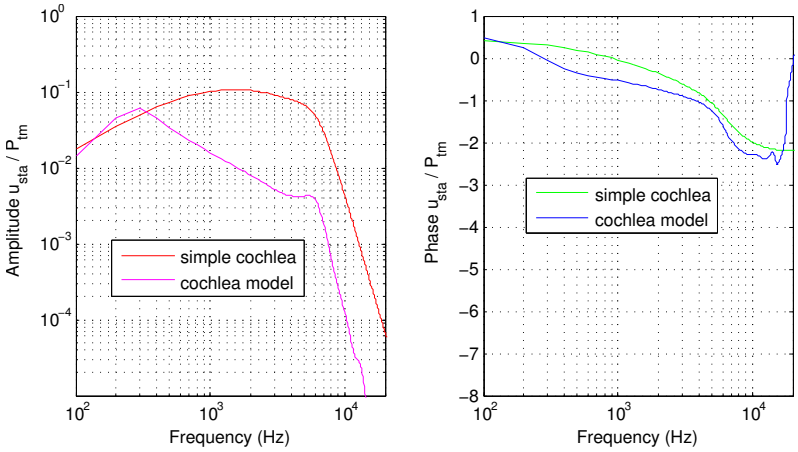

Figure 5.11: Amplitude and phase plots of the transfer functions of (1) the implicit ME model with *simple cochlea* and the implicit ME model with *implicit cochlea model* at a sample frequency of 320 kHz.

In both models, we are still measuring frequencies in the stapes. The amplitude plot (left) indicates a faster decay of the transfer function at higher frequencies. A possible explanation is the distance that waves from the stapes have to endure. The characteristic position of lower frequencies on the BM is more distant from the stapes than for higher frequencies. Effects on velocity formed at these positions have to endure more circuit elements which could cause more damping of these effects than the case where the whole cochlea is trapped in one element neighbouring the stapes. When frequencies get higher, these distances play a minor role and the transfer function tends to go back to the behaviour of the model with the simple cochlea. The difference of the total cochlea and a single resistor is also given in figure 17 of [2]. Only at a specific frequency or frequencies in the neighbourhood of this frequency a single resistor would be sufficient to model the transfer in the cochlea but covering the whole frequency spectrum is not possible.

The phase plot also shows a faster decay at lower frequencies and more similarity with the simple cochlea at higher frequencies. The places where the curves meet again is at the same frequency as for the amplitude plot at approximately 6 kHz followed by a quite similar behaviour. However, we see the phase going up again above 15 kHz. To avoid any misunderstading, the phase is not passing through zero at 20 kHz. The human cochlea is not able to detect frequencies above 20 kHz. The cochlea model and its parameters are based on these facts and therefore analysis of the model above 20 kHz is not relevant.

It is very important to keep in mind that the results above are not correct or wrong in a certain sense. There are different choices possible for the influence of the cochlea. The first model used one resistor with damping d_c to focus on the development of the ME model. The cochlea model itself uses a damping function $d(x)$ which is also a simplification since it only represents the linear part of the damping. Moreover, the ME model parameters are based on the fitting of data in [1]. Two model parts based on different articles (although very alike in approach) are glued together which could lead to some contradictions in the choice for parameters. As specified earlier, there are different choices for nonlinear damping functions which should be added to the linear damping. Further tweakening of the parameters could then be done by considering more audiological data.

5.4 Implementation of nonlinear damping

The damping is divided into a linear part and a nonlinear part. The linear part is based on $s(x)$ and for the nonlinear damping different choices exist. Remind from the mechanical oscillator the definition of the damping factor δ: $\delta = \frac{d}{\sqrt{ms}}$. With $s = s(x)$ from (3.26) and δ a given constant the damping becomes:

$$d(x) = d_L(x)d_{NL}(x) \text{ with } d_L(x) = \frac{\delta}{b\Delta X}\sqrt{m^s s_s(x)} = \frac{\delta}{b\Delta X}\sqrt{m^s s_0^s}e^{-\lambda x/2} \tag{5.9}$$

Definition 4 *A function f mapping an input variable $x(t)$ to an output variable $y(t)$ is linear if and only if for all constants α_1, α_2 and combination of inputs x_1, x_2 holds:*

$$f(\alpha_1 x_1 + \alpha_2 x_2) = \alpha_1 f(x_1) + \alpha_2 f(x_2) \tag{5.10}$$

□

The function f may also be interpreted as a linear system mapping an input signal $X(t)$ to an output signal $Y(t)$ by matrix multiplication. As long as these matrices are constant and the statement in definition 4 holds we consider linear systems. In particular in signal analysis, where linear systems play an important role, the mapping of the input $X(t)$ to the output $Y(t)$ is explicitly defined by a convolution product with the transfer function $H(t)$.

$$Y(t) = H(t) * X(t) = \int_{-\infty}^{\infty} H(\tau)X(t-\tau)d\tau \tag{5.11}$$

Calculations with integrals in convolution integrals could be very difficult and time consuming and therefore in signal analysis often the analysis is done in the frequency domain

by applying the Fourier transform $\mathcal{F}$. This has the big advantage of the property that if for example $X(\omega) = \mathcal{F}(x(t))$ the Fourier transform of $x(t)$, (5.11) is equivalent with:

$$Y(\omega) = H(\omega)X(\omega) \tag{5.12}$$

This result makes analysis much more easier if we transform the system to the frequency domain. A linear transfer function indicates per frequency the modification of the amplitude of the input and a possible delay T in the phase such that we can write:

$$y(t) = A \cdot x(t - T) \tag{5.13}$$

However, not every feature in signal processing can be explained by linear systems. An important example in cochlear modeling can be found in the concept of OAE's, explained in section 2. When a signal with more than one frequency is presented to the cochlea we are able to pick up a response containing frequencies which were absent in the stimulus. In the case of two frequencies f_1 and f_2 with $f_1 < f2$, a third frequency $2f_2 - f_1$ emerges. This is called the distortion product and and it is clearly formed by the processing in the cochlea. A linear transfer function described by (5.13) is obviously not able to generate distortion products which is a clue for *nonlinear processing in the cochlea.* OAE's formed by distortion products are called distortion product OAE's (DPOAE's) and are an excellent tool to study nonlinear behaviour of the cochlea [2]. Since we need nonlinear systems in cochlear modeling we do not have the comfort of the property in (5.12) anymore. Therefore, the development of the cochlea model should be done in the time domain. The advantage of time domain analysis is that model parameters which were chosen time-independent can now be adapted over time. It is the same idea as a feedback system where the systems transfer is adapted each timestep using the information of the previous timesteps. This brings us back to the nonlinear part d_{NL} of the damping d. Different choices for d_{NL} are possible to fit experimental data, some examples:

Van der Pol model [5]

$$d_{NL}(y) = 1 - y^2 \tag{5.14}$$

Duifhuis nonlinear damping [2]

$$d_{NL}(u) = \frac{\chi \sinh(\alpha u)}{\alpha u} - \frac{\gamma}{\cosh(\beta u)} \tag{5.15}$$

The proposed functions for d depend on the solutions for u or y which depend on time. Hence the value for d is being updated every timestep. The key concept of modeling active behaviour of the cochlea is the application of a nonlinear damping function. We will implement the nonlinear damping function proposed by van Hengel [2] in our new model and run tests to see whether we are able to model active behaviour. The nonlinear damping function is given:
A plot of this function is given in figure 5.12. The first problem we have to recognize is the time-dependence of the damping since $d(u) = d(u(t))$. If we move back to the solving process of the system where the Poisson equation and $u^{(n+1)}$ (see (4.33) and (4.32) in section 4.5) are solved. Since $\tilde{M}$ contains $d(u(t))$, the inverse of $K\tilde{M}^{-1}K^T$ has to be calculated each timestep instead of one time at the start of the process. This will have consequences for the amount of computations. In the case of the explicit method, d was

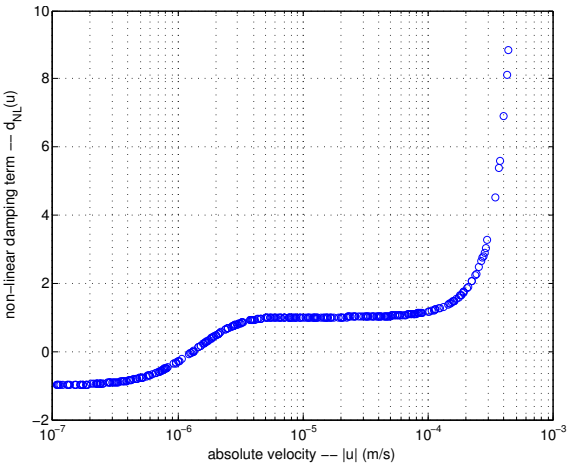

Figure 5.12: Plot of the nonlinear damping term with $\chi = 1$, $\alpha = 10^4$, $\beta = 10^6$ and $\gamma = 2$.

incorporated in the right hand side of the system. Although this right hand side should be recalculated every timestep, it is cheaper than the calculation of an inverse so this is really a downside of the implicit method. In practice however, the systems in cochlear modeling are not large since the amount of hair cells is on the BM is limited. Calculating the inverse matrices of size $N = 400$ every timestep is not a problem for computers nowadays.

The damping function is plotted for an interval of absolute values of $|u|$ that are relevant for the cochlear system. In this interval, the damping has a negative part and positive part. The velocity where the damping changes sign depends on the choice for the parameters in (5.15). We fix $\alpha = 10^4$ and by increasing β the intersection with the $|u|$-axis slides to the left. For the plot in figure 5.12, and in the rest of the paragraph, $\beta = 10^6$. The values of χ with respect to γ is important. At small velocities, the fraction with γ is dominant. If $\gamma > \chi$, negative damping will occur and active behaviour will arise. For now, we choose $\chi = 1$ and for the moment we set $\gamma = 0.5$ which implicates passive behaviour since $\gamma \leq \chi$. We follow [2] further by choosing the Greenwood place-frequency map:

$$f_r(x) = A \cdot 10^{-ax} - f_0 \tag{5.16}$$

with given constants A, a and f_0 (see the Appendix). The stiffness $s(x_i) = 4\pi^2 f_r(x_i)^2$ and the linear part of the damping is still coupled to the stiffness through the resonance relation $d_L(x_i) = \delta\sqrt{m \cdot s(x_i)}$ (see section 3.2). We run the model for both linear and nonlinear damping by presenting a stimulus with frequency 1000 Hz during 0.5 s. The Nyquist frequency is 6 kHz.
The first results are presented in figure 5.13. We measure the pressure (dB) in the ear canal and produce the frequency spectrum. The total time frame of 0.5 s is cut into fifty small frames (left plots) and the average of these frames is taken (right plots) to filter out events that do not occur on a regular basis. Clearly, we can see the difference that the nonlinear damping term brings. In both cases we see a clear peak at 1000 Hz coming from the stimulus and in the linear case further silence (the low-frequent behaviour does not have to be considered). The nonlinear plots on the contrary, seem to give more

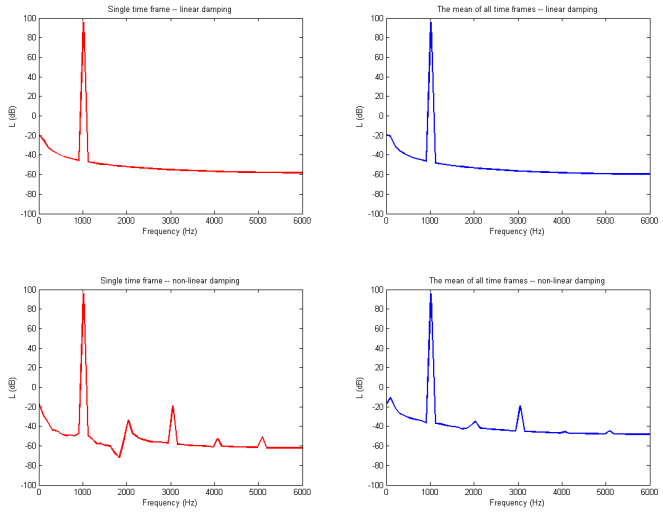

Figure 5.13: The occurence of distortion products in spectra of the pressure response at a stimulus of 1000 Hz.

peaks at multiples of 1000 Hz. These are the distortion products explained earlier this section which are directly linked with the theory of nonlinear behaviour. The peaks lie at multiples of 1000 Hz because of distortion of the stimulus with itself. The peaks of the products decay very fast but at odd multiples they are higher. This agrees with information about distortion products given by Duifhuis [5]. There is given a complex calculation for the amplitude of the peaks which we will not perform in this thesis. The most important result is that this is the first sign of nonlinear behaviour in the implicit model.

5.4.1 Active behaviour

To study active behaviour, we set a few positions next to each other at $\gamma > 1$ which will represent the active part of the cochlea. This idea is presented in [2] where $\gamma = 2$ is a regular choice, but we will choose γ more crude to detect active behaviour more easily. For the test phase of the model this is satisfied, for OAE simulations and real life results γ should be chosen more subtle. The frequency of active behaviour is chosen 1567 Hz (same as in [2]) and with (5.16) we determine its characteristic position to change γ.

We will run the model with no external stimulus presented to the ear. The velocities within the system are set randomly within the interval of figure 5.12 to give the system an initial energy. The model is ran for 4 s at the same Nyquist frequency (6 kHz) for different values of γ at the characteristic position where we also measure the velocity. We only have N=20 oscillators instead of the regular number of N=400 to save simulation time, the simulation will now only take approximately a minute, and $N = 20$ is sufficient to present active behaviour. The frequency spectra of the measurements are given in figure 5.14.

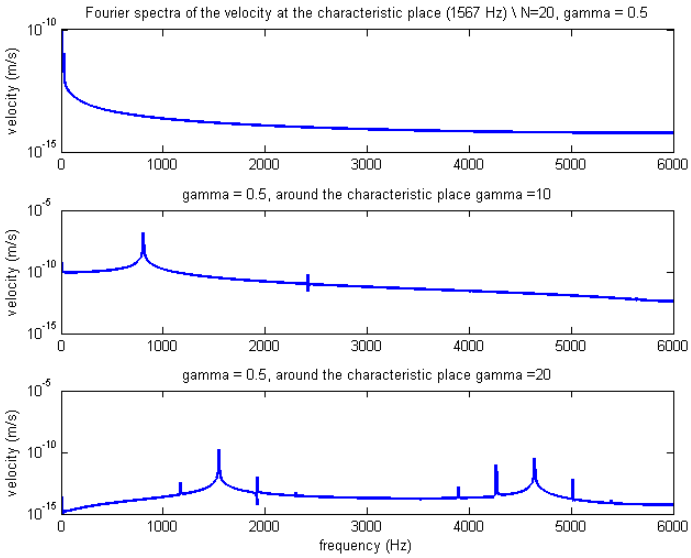

Figure 5.14: Spectra of velocity measurements at the characteristic position of $f_r = 1567Hz$. (upper) No active behaviour is set at f_r, $\gamma = 0.5$, (middle) the active behaviour is visible by setting $\gamma = 10$, (lower) the active behaviour is made more clear by increasing $\gamma = 20$

The first plot gives the situation of a totally passive cochlea. This spectrum is comparable with the spectra of figure 5.13 without the peak at 1000 Hz since we have no external stimulus. The second plot is the case of an active cochlea with $\gamma = 10$ at the characteristic position. Now we see the birth of frequencies at particular places due to the cochlear activity. Frequencies seem to gather at certain peaks where other frequencies just follow the original result. To emphasize this phenomenon a bit more, also a spectrum with $\gamma = 20$ is given in the third subplot. We see the peaks arising at the same frequencies and becoming more clear due to the stronger negative damping.
Since N is very low, not much information can be collected from the position of the peaks. Therefore, we present two equivalent simulations with $N = 200, 400$ to compare, see figure 5.15. We see that the peaks concentrate more around the dominant peaks. The location of the peaks seem to tend more to the characteristic frequency of 1567 Hz but it is not clear whether it actually converges to this frequency as N is increased.

The most important conclusion is the fact that our new model is capable of handling nonlinear damping functions to simulate active behaviour of the cochlea. By testing with crude choices for negative damping, we observed the formation of distortion products and the birth of peaks in the spectra where only a random initial velocity was applied. In the future, results could be tuned more to verify results with other work, for example in [2].

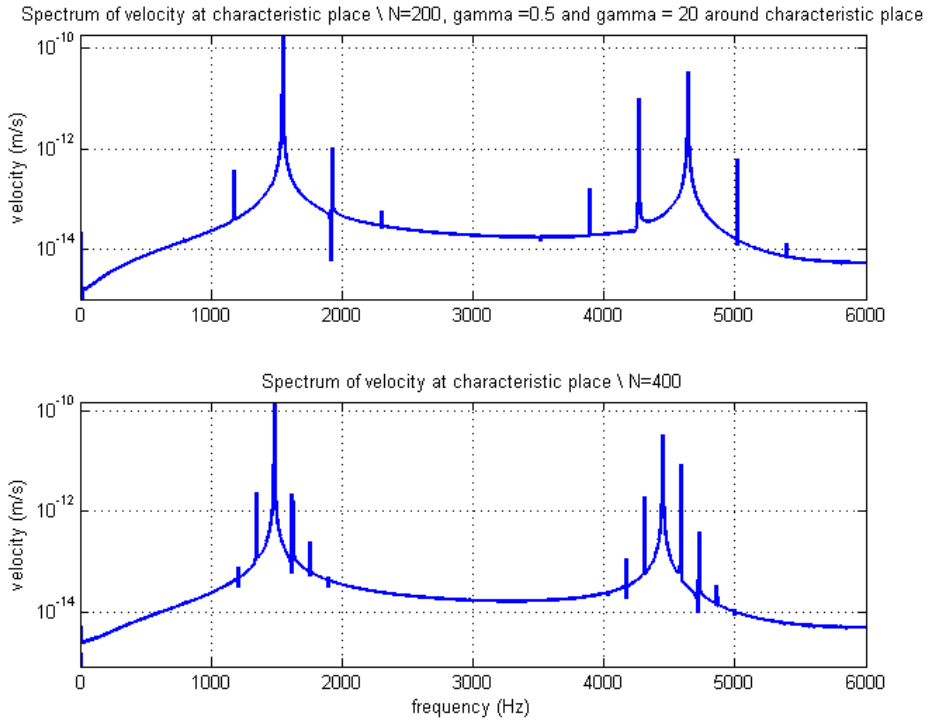

Figure 5.15: Spectra of the velocities Active behaviour at the characteristic position of $f_r = 1567Hz$ for a bigger amount of oscillators. (upper) $N = 200$, (lower) N=400

Chapter 6

Conclusion and future research

The objective of this thesis was to derive and implement a more detailed circuit model of the middle ear. The mathematical basis for the cochlea model has been laid by van den Raadt in [4]. To understand the mathematics behind cochlear modeling and to set up terminology we followed the approach of this article in great detail. With this knowledge of the cochlea we were able to couple the ME model presented by [1] to the cochlea model of [4].

Derivation of the set of circuit equations for the ME part in the same structure as for the cochlea turned out to be problematic. The mass term in the cochlea was absent in the ME equations due to the difference in physiology. This zero mass resulted in singularities in the ME equations. The mathematical translation of this problem is an algebraic constraint to the differential equations that govern the dynamics. This brought us to the theory of differential algebraic equations (DAE's) having its applications in a lot of other fields in engineering such as robotics.

The problem is solved however by choosing the time integration method before discretizing the circuit equations. Inspired by the theory from fluid dynamics, we replaced the explicit Euler method with an implicit Euler method for solving the differential equations in time which resulted in a reformulation of equations of the solving method. The zero mass was not causing singularities in the equations anymore, making the implicit method suitable for solving the ME equations.

Consequently, to be able to perform coupling with the ME, the cochlea model of [4] had to be rewritten in an implicit way first. The implicit cochlea model was implemented and verified with the original model by comparing simulation results from the cochlea model of INCAS^3. Solutions of both models seem to have problems at the boundaries implicating that these boundary conditions could be reconsidererd in the future, though results at the resonance do not seem to be influenced by the boundary effects. Finally, some bounds were specified to the mesh size and timestep to secure numerical stability and convergence of the results.

The ME model was derived and implemented in the same implicit structure as for the cochlea. Its correctness was verified by the simulation results presented in [1]. The implementation of the tympanic membrane had to be studied in more detail since its model

structure was not given explicitly in [1]. We chose to model the membrane as a single transmission line based on the suggestion by [7].

The two implicit models for the cochlea and the ME were then coupled and some results were presented to indicate the effects of the coupling. The most important functionality for future research is to be able to model OAE's and therefore we have sought to show the capabilities of the new model on this subject. A nonlinear damping function was implemented in the implicit model to verify whether the model is capable of simulating an active cochlea, the origin of OAE's. Results of simulations show signs of an active cochlea making the new model suitable for research to OAE's. These results however are still rough indications and relative high negative damping coefficients have been chosen to provide clear results. The simulation results are quite raw and audiological knowledge will have to extend the research to obtain a better interpretation of the results. In the future, the model should be polished to get more subtle results which can be verified with the simulation results of nonlinear cochlae in [2]. Especially, the parameters of the tympanic membrane could be tuned since the choice for these parameters is accurate up to an order of magnitude.

The implementation of the ME model is based on the simplest implicit time integration method we know, the Backward Euler Method. The simplicity and its implicit structure were ideal to develop the implicit ME and cochlea model. More options for implicit time integration methods could be investigated in the future to optimize the solving process. This could lead to more accurate results and better numerical efficiency.

In audiology, the development of a time domain cochlea model has made some progress. The ME is written out in more mechanical elements representing the functionality of each individual element much better. More parameters can now be varied to investigate their individual influence on the simulation results and optimized to fit experimental data. Inspired by other fields in engineering like fluid dynamics and electronics, we introduced the implicit method in cochlear modeling for the sake of improvement of solving the middle ear model.

Appendix A

Tables of constants and parameters

Constant	Value	Unit	Description
L	$35 * 10^{-3}$	m	Length of the cochlea
b	$1 * 10^{-3}$	m	Width of the basilar membrane
h	$1 * 10^{-3}$	m	Height of the SV and ST
N	400		Number of oscillators in cochlea
A_{st}	$3 * 10^{-6}$	m^2	Area of the stapes
A_t	$60 * 10^{-6}$	m^2	Area of the eardrum
ρ	$1 * 10^3$	$\frac{kg}{m^3}$	Density of cochlear fluid
m^s	0.5	$\frac{kg}{m^2}$	The specific acoustic mass in the cochlea
δ	$5 * 10^{-2}$		The damping factor in the cochlea
ω_{rm}	$2\pi * 2000$	$\frac{rad}{s}$	Resonance frequency of the ME
δ_m	2.5		Damping factor at the ME
n_t	30		Transformation factor of the ME
Z_a^s	415	$\frac{Ns}{m^3}$	Specific acoustic impedance of air
$\hat{t_0}$	$1 * 10^{-3}$	s	Characteristic time
$\hat{y_0}$	$1 * 10^{-9}$	m	Characteristic length in y-direction
$\Delta\tilde{X}_0$	$\frac{1}{400}$		Dimensionless distance between ME and first oscillator
λ	300	m^{-1}	Parameter for the relation between place and stiffness
s_0^s	$1 * 10^{10}$	$\frac{kg}{m^2 s^2}$	Specific acoustic stiffness constant

Symbol	Formula	Unit	Description
A_v	bh	m^2	Area of the scalae
$\Delta\tilde{X}$	$\frac{1}{N}$		Dimensionless distance between two oscillators
Δt		s	Timestep in time integration
u		$\frac{m}{s}$	Velocity
y	$\frac{\partial u}{\partial t}$	m	Displacement
q		$\frac{m^3}{s}$	Flux or volume velocity
Y	$\frac{\partial q}{\partial t}$	m^3	Volume displacement
p		$\frac{kg}{ms^2}$	Pressure
m	$\frac{m^s}{bL\Delta\tilde{X}}$	$\frac{kg}{m^4}$	Acoustic mass
m_c	$\frac{\rho\Delta\tilde{X}}{bh}$	$\frac{kg}{m^4}$	Acoustic mass of cochlear fluid
m_{c0}	$\frac{\rho L\Delta\tilde{X}_0}{h}$	$\frac{kg}{m^4}$	Acoustic mass of cochlear fluid at the ME
m_h	$\frac{\pi\rho}{2b}$	$\frac{kg}{m^4}$	Acoustic mass of the helicotrema
m_m	$\frac{n_t^2 Z_a}{\omega_{rm}\delta}$	$\frac{kg}{m^2}$	Acoustic mass of the ME
d		$\frac{kg}{m^4 s}$	Acoustic damping
d_m	$n_t^2 Z_a$	$\frac{kg}{m^4 s}$	Acoustic damping of the ME
s		$\frac{kg}{m^4 s^2}$	Acoustic stiffness
s_m	$\frac{d_m^s \omega_{rm}}{\delta}$	$\frac{kg}{m^4 s^2}$	Acoustic stiffness of the ME
Z_a	$\frac{Z_a^s}{A_t}$	$\frac{Ns}{m^5}$	Acoustic impedance of air
m_c^s	$\frac{\rho L^2\Delta\tilde{X}^2}{h}$	$\frac{kg}{m^2}$	Specific acoustic mass of cochlear fluid
m_{c0}^s	$\frac{\rho L\Delta\tilde{X}_0}{h}$	$\frac{kg}{m^2}$	Specific acoustic mass of cochlear fluid at the ME
m_h^s	$\frac{\pi\rho L\Delta\tilde{X}}{2}$	$\frac{kg}{m^2}$	Specific acoustic mass of the helicotrema
m_m^s	$\frac{n_t^2 Z_a bL\Delta\tilde{X}}{\omega_{rm}\delta}$	$\frac{kg}{m^2}$	Specific acoustic mass of the ME
d^s		$\frac{kg}{m^2 s}$	Specific acoustic damping
d_m^s	$n_t^2 Z_a bL\Delta\tilde{X}$	$\frac{kg}{m^2 s}$	Specific acoustic damping of the ME
s^s		$\frac{kg}{m^2 s^2}$	Acoustical stiffness
s_m^s	$\frac{d_m^s \omega_{rm}}{\delta}$	$\frac{kg}{m^2 s^2}$	Specific acoustic stiffness of the ME

Appendix B

Matrices for the implicit total ear model

To visualize the structure of the matrices in implicit circuit model equations, the matrices for the implicit total ear model are given below. The matrices of the implicit cochlea and middle ear model are submatrices of the ones for the total ear.

- $M = \text{diag}\begin{pmatrix} m_{tm} \\ 0 \\ m_{mal} \\ 0 \\ m_{inc} \\ 0 \\ m_{sta} \\ m \\ 2m_c \\ m \\ 2m_c \\ \vdots \\ m \\ 2m_c \\ m \\ 2m_c + m_h \end{pmatrix}, D = \text{diag}\begin{pmatrix} 0 \\ 0 \\ d_{mal} \\ d_{IM} \\ 0 \\ d_{IS} \\ d_{sta} \\ d_1 \\ 0 \\ d_2 \\ 0 \\ \vdots \\ d_{N-1} \\ 0 \\ d_N \\ 0 \end{pmatrix}, S = \text{diag}\begin{pmatrix} 0 \\ s_{tm} \\ s_{mal} \\ s_{IM} \\ 0 \\ s_{IS} \\ s_{sta} + s_{RW} \\ s_1 \\ 0 \\ s_2 \\ 0 \\ \vdots \\ s_{N-1} \\ 0 \\ s_N \\ 0 \end{pmatrix} \in \mathbb{R}^{(2\text{N}+7)\cdot(2\text{N}+7)}$
- $\mathbf{e}^{(n)} = \begin{pmatrix} -\frac{n_t dt}{m_m + d_m dt + s_m dt^2} p_{tm}^{(n)} \\ 0 \\ \vdots \\ 0 \end{pmatrix} \in \mathbb{R}^{N+3}$

Appendix C

Matlab code of the developed models

```
% An implementation of the implicit middle ear model coupled with the
    implicit cochlea model
%
%
% Author:   Oscar Heslinga
% Version:  0
% Date:     24/9/2013
% Copyright:      INCAS3, The Netherlands
%
%
%
% input_parameters:
%
% - t_end: Total time of simulation in seconds (real time)

function [] = total_ear_model(t_end);

    % Parameter list (based on Table 1 O'Connor and Puria

            b = 1e-3;           % [m] width scalae (page 19)
            L = 35e-3;          % Length of the cochlea
            h = 1e-3;           % [m] height of scalae (page 3)
            S_sc = 1e-6;        % [m^2]cross sectional area of the cochlea
            rho = 1e3;          % [kg/m^3] density of cochlear fluid
            m_s = 0.5;          % [kg/m^2] specific acoustic mass BM
            s_st = 3e-6;        % [m^2] area of a segment (stape)
            S_t = 60e-6;        % [m^2] area of eardrum
            omega_rm= 2*pi*2000; % [rad/s] resonance frequency of midear
            delta = 2.5;        % reciprocal of the Q factor of the midear
            n_t = 30;           % transformation factor of the midear
            Z_s = 415;      % [Ns/m^3] Specific acoustic impedance of air
            p_ref = 2e-5;       % [Pa] reference pressure, equals 0 dB SPL
            s_0 = 1e10;    % [Pa/m] specific acoustic stiffness constant
            lambda = 300;       % [/m] parameter for frequency-place map
            epsilon = 5e-2;     % modulation factor for a resonator

    % Parameters in the middle ear

            A_tm = 6.0e-5;      % [m^2] Area of the TM
```

```
  % Estimated parameters for the TM
      m_tm = 1e3;          % [kg/(m^4)] acoustic mass of TM
      s_tm = 1e12;         % [kg/(s^2m^4)] acoustic stiffness of TM

      m_mal = 3.24e-6;     % [kg] mass of the malleus
      d_mal = 0.140;       % [kg/s] damping of the malleus
      s_mal = 504;         % [kg/s^2] stiffness of the malleus
      N_LR = 1.3;          % Lever ratio of the IM joint
      d_IM = 4.56e-2;      % [kg/s] damping of the IM joint
      s_IM = 1.46e3;       % [kg/s^2] stiffness of the IM joint
      m_inc = 7.30e-6;     % [kg] mass of the incus
      d_IS = 3.04e-2;      % [kg/s] damping of the IS joint
      s_IS = 10.0e3;       % [kg/s^2] stiffness of the IS joint
      A_fp = 3.14e-6;      % [m^2] Area of the stapes footplate
      m_sta = 3.55e5;      % [kg/m^4] acoustic mass stapes
      d_sta = 1e10;        % [kg/(sm^4)] acoustic damping stapes
      s_sta = 0.81e14;     % [kg/(s^2m^4)] acoustic stiffness stapes
      s_RW = 0.3e14;       % [kg/(s^2m^4)] acoustic stiffness RW
      d_c = 1.99e10;       % [kg/(sm^4)] acoustic damping cochlea
      p_ref = 2e-5;        % [Pa] reference pressure, equals 0 dB SPL

% Determine whether we want to use dimensionless variables
% (only possible for the cochlea model yet)

  set_dimless = 0;

      if set_dimless == 1 % Dimensionless variables

            t_0_hat = 1e-3;     % [s] characteristic time scale
            x_0_hat = 35e-3;    % [m] characteristic length scale
            y_0_hat = 1e-9;     % [m] characteristic amplitude scale

      else                % No dimensionless variables

            t_0_hat = 1;        % [s]
            x_0_hat = 1;        % [m]
            y_0_hat = 1;        % [m]

      end

% Grid settings

      freq_max = 6e3;               % [Hz] The Nyquist frequency
      dt = 1/(2*freq_max*t_0_hat);  % [s] time step (1/samplefreq)
      t_stim = 0:dt:t_end;          % Set up grid in time
      N_t_stim = length(t_stim);    % Time stages stimulus
      t_part = 0.05;                % cut time grid in frames
                                    % for non-linear analysis
      N_t_part = floor(t_part./dt); % Time stages in frame
      N = 400;                      % Grid cells cochlea
      dx_01 = L/(N*x_0_hat);        % midear segment length
      dx = (L-dx_01-h)/(N*x_0_hat); % length of segment in cochlea
      x  = [ 0, dx_01 : dx : ...    % the place vector
            (L-h)/x_0_hat];
      u  = zeros( 2*N+7, 1 );       % initial velocity vector
      y  = zeros( 2*N+7, 1 );       % initial displacement vector
      y_ref = zeros( N,1 );         % zero reference line for plot
```

```
      p  = zeros( N+4, 1);          % initial pressure vector

% Parameters for the logartithmic Greenwood place-frequency map

      a = 65.1;                     % [/m]
      A_g = 17.927e3;               % [Hz]
      f_0 = 145.4;                  % [Hz]
      f_OAE = 1567;                 % [Hz] Frequency where OAE can
                                    % be detected in Greenwood map
      beta_OAE = 0.1e6;             % beta value for the place
                                    % where an OAE can be detected
      gamma_OAE = 20;               % gamma value for the place
                                    % where an OAE can be detected

% Parameters for the non-linear damping term

      alpha = 1e4;
      beta  = 1e6;
      gamma = 2;
      chi   = 1;

% Greenwood place-frequency map

      f_r = A_g*10.^(-a.*x(2:N+1)) - f_0;

% Transformation parameters to the acoustic domain, middle ear part

      m_mal = m_mal/A_tm.^2;  % [kg/m^4] acoustic mass malleus
      d_mal = d_mal/A_tm.^2;  % [kg/sm^4] acoustic damping malleus
      s_mal = s_mal/A_tm.^2;% [kg/s^2m^4] acoustic stiffness malleus
      d_IM = d_IM/(A_tm*N_LR).^2; % [kg/sm^4] acoustic damping IM
      s_IM = s_IM/(A_tm*N_LR).^2; % [kg/s^2m^4]acoustic stiffness IM
      m_inc = m_inc/(A_tm*N_LR).^2; % [kg/m^4] acoustic mass incus
      d_IS = d_IS/(A_tm*N_LR).^2; % [kg/sm^4] acoustic damping IS
      s_IS = s_IS/(A_tm*N_LR).^2;% [kg/s^2m^4] acoustic stiffness IS

% Acoustic with middle ear transformers taken into account

      m_sta = m_sta*A_fp.^2/(A_tm*N_LR).^2; % [kg/m^4] acoustic mass
                                            % of the stapes
      d_sta = d_sta*A_fp.^2/(A_tm*N_LR).^2; % [kg/sm^4]acoustic
                                            % damping of the stapes
      s_sta = s_sta*A_fp.^2/(A_tm*N_LR).^2; % [kg/(s^2m^4)] acoustic
                                            % stiffness stapes
      s_RW = s_RW*A_fp.^2/(A_tm*N_LR).^2;   % [kg/(s^2m^4)] acoustic
                                            % stiffness round window
      d_c = d_c*A_fp.^2/(A_tm*N_LR).^2;     % [kg/(sm^4)] acoustic
                                            % damping of the cochlea

% Further acoustic mass, damping and stiffness in cochlea

      m_h = rho*pi/(2*b);
      m_c = (rho*x_0_hat*dx)/h;
      m_s = m_s/(b*x_0_hat*dx);

% Set up grid for the time stages to plot or write data

      t = 0:dt:t_end;         % Set column vector for the time
```

```
N_t = length(t);        % Number of timestages

number_plots = 10;      % Number of stages user wants plot
plot_time = floor(N_t/number_plots); % Time stage for a plot
number_frames = 50;
frame_time = floor(N_t/number_frames); % Time one time frame
frame_nr = 1;

% Construction of external stimulus

signal_type = 'diracdelta';   % Choose the type of stimulus

if signal_type == 'puresignal' % Stimulus one frequency signal

      omega_1     = 1;  % parameter to smooth-start the signal
      f_1   = 1000;     % [Hz] frequency of the signal
      L_dB  = 60;       % Sound pressure of stimulus in dB
      p_AM1 = p_ref*10^(L_dB/20);   % [Pa]

      % The input stimulus during one time frame

      p_e(1:N_t_part,1) = ...
            p_AM1*omega_1*sin(2*pi*f_1*t_stim(1:N_t_part));
      p_e(N_t_part+1:N_t_stim) = 0;

elseif signal_type == 'diracdelta'  % Stimulus Dirac function

      p_e = zeros(N_t_stim,1);
      p_e(5)=10;

elseif signal_type == 'whitenoise'  % Stimulus is white noise

      p_e(1:N_t_stim,1) = wgn(N_t_stim,1,60,'dBW');
      p_e = p_ref*p_e;      % Transfer units dB Volt to dB SPL

elseif signal_type == 'nostimulus'

      p_e = zeros(N_t_stim,1);      % No stimulus is presented

end

% A random initial velocity is chosen to put energy into the system

u(8:2:2*N+7,1) = ...
            randn(N,1).*sort(b*dx*([10.^(-7+4*rand(N,1))]));

% Place mass, damping and stiffness in vector form

m(1:7,1)= [m_tm 0 m_mal 0 m_inc 0 m_sta];
m(8:2:2*N+7,1) = [m_s];
m(9:2:2*N+7,1) = [2*m_c];
m(2*N+7,1) = [2*m_c+m_h];

s(1:7,1) = [0 s_tm s_mal s_IM 0 s_IS s_sta+s_RW];
s(8:2:2*N+7,1) = m_s*4*pi.^2*f_r.^2;
s(2*N+7,1) = 0;

d(1:7,1) = [0 0 d_mal d_IM 0 d_IS d_sta];
```

```
        d(2*N+7,1) = 0;

    % Linear damping function

        d_L(8:2:2*N+7,1) = epsilon*sqrt(m_s*s(8:2:2*N+7,1));

% set the gnuplot toolkit if working in Octave @ INCAS3
% graphics_toolkit('gnuplot');

% Loop through the simulation process

disp('start of simulation');

for n = 1:N_t

% Column vectors for damping which are non-linear

    d_NL(1:N,1) = chi*sinh(alpha.*u(8:2:2*N+7,1)./(b*dx))...
                    ./(alpha.*(u(8:2:2*N+7,1)./(b*dx)))
                    - gamma./(cosh(beta.*u(8:2:2*N+7,1)./(b*dx)));

    % Option to locate an other value for beta at a certain frequency

    x_OAE = (-1/a)*log10((f_OAE+f_0)/A_g);  % position in the cochlea
                                            % where f_OAE resides
                                            % according to Greenwood
    [x_OAE_approx,x_OAE_ind] = min(abs(x-x_OAE)); % Determine index of
                                                  % the element in x
                                                  % closest to x_OAE


    % Set active part in non-linear damping
    d_NL([x_OAE_ind-1:x_OAE_ind+1],1) = ...
        chi*sinh(alpha.*u(8+2*(x_OAE_ind-1),1)./(b*dx))...
        ./(alpha.*(u(8+2*(x_OAE_ind-1),1)./(b*dx))) - ...
        gamma_OAE ./(cosh(beta_OAE.*u(8+2*(x_OAE_ind-1),1)/(b*dx)));


    d(8:2:2*N+7,1) = d_L(8:2:2*N+7,1).*d_NL; % Update damping function

% Construction of system matrices

        % Construction of M and S

              for i = 1:2*N+7

                    M_tilde_inv(i,i) = 1./(m(i)+ d(i)*dt+s(i)*dt.^2);

              end

              M = diag(m);
              S = diag(s);

        % Construction of K and G

              for i = 1:N+3

                    K(i,2*i-1:2*i+1) = [-1 1 1];
```

```
            end

        % Input construction

            e = zeros(2*N+7,1);
            I = eye(2*N+7);

        % Construction of iteration matrix of q

            A = dt*K*M_tilde_inv*K';
            invA = inv(A);

        % Input pressure of the system

            e(1,1) = dt*M_tilde_inv(1,1)*(p_e(n));

        % Poisson equation and implicit update of u

            p = -invA*K*(M_tilde_inv*M*u - dt*M_tilde_inv*S*y + e);

            u = M_tilde_inv*(M*u + dt*K'*p - dt*S*y) + e;

        % Implicit time integration of discplacement

            y = y + dt*u;

        % Write velocity, pressure and displacement cochlea entrance
        % in vector for later analysis

        v_st(n,1) = u(7,1)*1e3/(A_tm*N_LR);
        p_EC_column(n-frame_time*(frame_nr-1),1) = p(1,1);
        u_data(n,1:3) = [u(x_OAE_ind,1) u(1,1) u(8,1)];

        % Plot lines for u,y during simulation

        if rem( n , plot_time ) == 0 || n==N_t

            subplot(2,1,1), plot(x(2:end-1)', u(8:2:2*N+7,1), ...
            'g', x(2:end-1)', y(8:2:2*N+7,1), 'r', x(2:end-1)'...
            , y_ref, 'k');

            title( sprintf('Implicit progress %.2f steps, ...
            N = %.2f, t = %.2f ', n, N, t(n) ) );
            axis('tight');
            drawnow;
            pause(0.5);
        end

    end

    if rem( n , frame_time ) == 0

        p_EC(:,frame_nr) = p_EC_column;
        frame_nr = frame_nr + 1;

    end
```

```
      % Analysis and plot lines of transfer functions

            % Fourier transform the input pressure and output velocity

                  p_e_four = fft(p_e);
                  v_st_four  = fft(v_st);

            % Calculate transfer function (amplitude and phase)

                  G_ME_amp = abs(v_st_four./p_e_four);
                  G_ME_phase = angle(v_st_four./p_e_four);

            % Set frequency axis to the Nyquist frequency

                  f = N_t_stim/(2*t_end)*linspace(0,1,N_t_stim/2+1);

      % Amplitude of transfer function

            subplot(2,1,1), loglog(f,G_ME_amp(1:N_t_stim/2+1),'r');
            axis([100 20000 1e-5 1]);
            grid on;

      % Phase of transfer function

            subplot(2,1,2), semilogx(f,G_ME_amp(1:N_t_stim/2+1),'r');
            axis([100 20000 -8 1]);
            grid on;

      disp('end of simulation');

end
```

Bibliography

[1] Kevin N. O'Connor & Sunil Puria, *Middle-ear circuit model parameters based on a population of human ears*, Journal of the Acoustical Society of America, Vol. 123, No.1, January 2008

[2] P.W.J. van Hengel, *Emissions from cochlear modelling*, PhD thesis, 1996

[3] A.E.P. Veldman, *Computational Fluid Dynamics*, Lecture notes in Applied Mathematics, January 2012

[4] M. van der Raadt, *Formulering 1-dimensionaal cochlea model in termen van een netwerk (naar H. Duifhuis)*, 1991

[5] H. Duifhuis, *Cochlear Mechanics: Introduction to a Time Domain Analysis of the Nonlinear Cochlea*, (Springer, New York) 2012

[6] E. de Boer & M.A. Viergever, *Mechanics of Hearing, Proceedings of the IUTAM/ICA symposium*, 1983

[7] Sunil Puria & Jont B. Allen, *Measurements of the cat middle ear: Evidence of tympanic membrane acoustic delay*, Journal of the Acoustical Society of America, Vol. 104, No. 6, December 1998

[8] Békésy G. *Experiments in Hearing* (McGraw-Hill, New York), 1960

[9] Linda R. Petzold, *Numerical solutions of differential-algebraic equations in mechanical systems simulations*, Physica D 60 pp 269-279 , 1992

[10] R. Costa-Castelló, R. Griño, L. Basañez, *DAE Methods in Constrained Robotics Simulation*, Computación y Sistemas Vol. 1 No. 3 pp 145-160, 1998

[11] K. Lindenberg, P.W.J. van Hengel, *Stability analysis in a model of the human inner ear*, Bachelor thesis in Applied Mathematics, 2013

[12] Wolff, R *Hearing screening in newborns: systematic review of accuracy, effectiveness, and effects of interventions after screening.*, Archives of disease in childhood [0003-9888] yr:2010 vol:95 iss:2 pg:130 -135

Acknowledgements

After finishing this piece of academic work, satisfied and a bit relieved, I would like to thank a set of people that have made a significant contribution to my thesis. In a direct academic way, or implicitly, by any kind of support. First of all, I am very grateful to prof. dr. Arthur Veldman who has been my first supervisor and the person with the idea to connect my research interests to the project proposal that resulted in this thesis. Though my research was stretching a lot of physical fields, from audiology to electronics to fluid dynamics, he managed to translate my questions to his own expertise and came up with understandable solutions and ideas that were essential for the progress of my research. Second is dr. ir. Peter van Hengel who has been my supervisor at INCAS^3. He was able to present a problem from cochlear modeling in a project proposal that aroused my interests as a student in mathematics. He also had the task to translate my mathematical results into his experience in audiology and steer into the right direction which he managed to do quite well. New ideas and criticism from my supervisors kept me motivated to improve my work. I have spent some days working with ir. Bert Maat from the ENT department of the UMCG. I want to thank him for sharing his knowledge on the cochlea model and showing me the daily work of an audiologist at the hospital. His tour through the department and the stories about working with patients with cochlear implants have been an inspiration. I want to thank the research institute INCAS^3 in Assen which facilitated in working as a young academic researcher in a field full of applications during a 12-month internship. Especially, dr. Dirkjan Krijnders who helped me with my daily questions at INCAS^3 about the cochlea model and many other technical problems. And of course the rest of my colleagues at INCAS^3 who provided a nice working atmosphere and shared their work through interesting discussions and seminars. Not to forget my study mates at the university for a good time and study association FMF for the free coffee and organizing a three week sabbatical to South Africa during my master thesis. Last but not least my parents of course, who have supported me both mentally and financially not only during my master thesis but throughout my whole period of studying at the University of Groningen. Thank you all!